Impaired SMAD1/5 mechanotransduction and Cx37 (connexin37) expression enable pathological vessel enlargement and shunting

Peacock, Hanna M; Tabibian, Ashkan; Criem, Nathan; Caolo, Vincenza; Hamard, Lauriane; Deryckere, Astrid; Haefliger, Jacques-Antoine; Kwak, Brenda; Zwijsen, An; Jones, Elizabeth A V

How to cite

PEACOCK, Hanna M et al. Impaired SMAD1/5 mechanotransduction and Cx37 (connexin37) expression enable pathological vessel enlargement and shunting. In: Arteriosclerosis, Thrombosis, and Vascular Biology, 2020, vol. 40, n° 4, p. e87–e104. doi: 10.1161/ATVBAHA.119.313122

This publication URL: https://archive-ouverte.unige.ch/unige:131414
Publication DOI: 10.1161/ATVBAHA.119.313122

Arteriosclerosis, Thrombosis, and Vascular Biology

ORIGINAL RESEARCH

Impaired SMAD1/5 Mechanotransduction and Cx37 (Connexin37) Expression Enable Pathological Vessel Enlargement and Shunting

Hanna M. Peacock, Ashkan Tabibian, Nathan Criem, Vincenza Caolo, Lauriane Hamard, Astrid Deryckere, Jacques-Antoine Haefliger, Brenda R. Kwak, An Zwijsen, Elizabeth A.V. Jones

OBJECTIVE: Impaired ALK1 (activin receptor–like kinase-1)/Endoglin/BMP9 (bone morphogenetic protein 9) signaling predisposes to arteriovenous malformations (AVMs). Activation of SMAD1/5 signaling can be enhanced by shear stress. In the genetic disease hereditary hemorrhagic telangiectasia, which is characterized by arteriovenous malformations, the affected receptors are those involved in the activation of mechanosensitive SMAD1/5 signaling. To elucidate how genetic and mechanical signals interact in arteriovenous malformation formation, we sought to identify targets differentially regulated by BMP9 and shear stress.

APPROACH AND RESULTS: We identify Cx37 (Connexin37) as a differentially regulated target of ligand-induced and mechanotransduced SMAD1/5 signaling. We show that stimulation of endothelial cells with BMP9 upregulated Cx37, whereas shear stress inhibited this expression. This signaling was SMAD1/5-dependent, and in the absence of SMAD1/5, there was an inversion of the expression pattern. Ablated SMAD1/5 signaling alone caused arteriovenous malformation–like vascular malformations directly connecting the dorsal aorta to the inlet of the heart. In yolk sacs of mouse embryos with an endothelial-specific compound heterozygosity for *SMAD1/5*, addition of TNFα (tumor necrosis factor-α), which downregulates Cx37, induced development of these direct connections bypassing the yolk sac capillary bed. In wild-type embryos undergoing vascular remodeling, Cx37 was globally expressed by endothelial cells but was absent in regions of enlarging vessels. TNFα and endothelial-specific compound heterozygosity for *SMAD1/5* caused ectopic regions lacking Cx37 expression, which correlated to areas of vascular malformations. Mechanistically, loss of Cx37 impairs correct directional migration under flow conditions.

CONCLUSIONS: Our data demonstrate that Cx37 expression is differentially regulated by shear stress and SMAD1/5 signaling, and that reduced Cx37 expression is permissive for capillary enlargement into shunts.

Key Words: aorta ■ arteriovenous malformation ■ Connexin37 ■ endothelial cells ■ vascular remodeling

Blood vessels are dynamically remodeled throughout life in response to both molecular signals and changes in blood flow, thereby allowing them to adapt the vascular supply to the current needs of a tissue. Failed vascular remodeling can result in vascular malformations, including arteriovenous malformations (AVMs). AVMs are direct shunts between arteries and veins, bypassing the capillary bed.[1] AVMs are a defining characteristic of the human disease hereditary hemorrhagic telangiectasia (HHT), which is caused by autosomal dominant mutations in the ALK1 (activin receptor–like kinase-1)/Endoglin signaling pathway. To date, HHT-linked mutations have been identified for Endoglin (also called CD105), ALK1, their ligand BMP9 (bone morphogenetic protein 9, encoded by *GDF2*), or the downstream signaling mediator SMAD4.[2–5]

Correspondence to: Elizabeth A.V. Jones, Department of Cardiovascular Sciences, KU Leuven, UZ Herestraat 49 box 911, 3000 Leuven, Belgium. Email liz.jones@kuleuven.be

The online-only Data Supplement is available with this article at https://www.ahajournals.org/doi/suppl/10.1161/ATVBAHA.119.313122.

For Sources of Funding and Disclosures, see page xxx.

Arterioscler Thromb Vasc Biol is available at www.ahajournals.org/journal/atvb

Nonstandard abbreviations and acronyms

αSMA	α-smooth muscle actin
ALK	activin receptor–like kinase-1
AVM	arteriovenous malformation
BMP	bone morphogenetic protein
Cx37	connexin 37, encoded by GJA4
dHet^{EC}	mice with endothelial-specific heterozygous deletion of SMAD1/5
dKO^{EC}	mice with endothelial-specific deletion of SMAD1/5
E	embryonic day
EC	endothelial cell
FBS	fetal bovine serum
HHT	hereditary hemorrhagic telangiectasia
HMvEC	human microvascular endothelial cell
HUVEC	human umbilical vein endothelial cell
KOSR	knockout serum replacement
LDL	low-density lipoprotein
TGFβ	transforming growth factor-β
TNFα	tumor necrosis factor-α

Highlights

- Shear stress can upregulate or downregulate Cx37 (Connexin 37) depending on the ALK1 (activin receptor–like kinase-1)-binding ligands that are present in the media.
- SMAD1/5 endothelial-specific knockout embryos present with vascular defects connecting the dorsal aorta to the inlet of the heart, whereas heterozygotes can be induced to develop these malformations by the additional of TNFα (tumor necrosis factor).
- Localized loss of Cx37 is permissive for shunt formation when other mechanosensitive pathways are also disrupted.

The type I BMP receptor ALK1 is highly enriched in endothelial cells (ECs).[6] In response to the ligands BMP9, BMP10, and TGFβ (transforming growth factor-β), ALK1, in complex with a type II receptor (eg, BMPRII), induces phosphorylation of the intracellular effector proteins, SMAD1/5/9.[7] Phosphorylated SMAD1/5/9 associates with SMAD4 in a heterotrimeric complex. This complex translocates into the nucleus and binds to BMP-response elements to modulate gene expression.[8] SMAD1/5/9 signaling is necessary for induction of genes involved in vascular remodeling, including *Msx1*, *Id1*, and *Tmem100*.[9–11] Endoglin, the co-receptor for ALK1, is primarily expressed on ECs and is required for SMAD1/5/9 phosphorylation in response to BMP9.[12] Embryos lacking *Eng* (encoding for Endoglin), *Acvrl1* (encoding for ALK1), *Bmpr2*, or *Smad1/5* (either compound heterozygosity or an EC-specific loss of all 4 alleles) die at mid-gestation with a failure of vascular remodeling.[13–17] Mice heterozygous for *Alk1* or *Eng* survive to adulthood but develop AVMs, though with incomplete penetrance.[16,18]

Shear stress induces SMAD1/5/9 phosphorylation in an ALK1/Endoglin-dependent manner, in the presence of ligand.[19] Shear stress-signaling via the ALK1 signaling pathway is critical for pericyte recruitment, restraining EC proliferation, regulating direction and speed of EC migration, governing EC shape, and preventing excessive vessel dilation in response to flow.[20–24] The fact that HHT is caused by mutations in shear stress–sensitive components upstream of SMAD1/5/9 signaling has led to the hypothesis that AVMs develop due to impaired mechanotransduction.

In animal models and in HHT patients, the ALK1/Endoglin/SMAD1/5/9 signaling pathway is disrupted throughout the entire vascular system, yet AVMs are a localized phenomenon. Hence, genetic factors alone cannot explain AVM formation—a local factor has been proposed to be required for AVM formation. Here we show that shear stress–induced SMAD1/5/9 signaling regulates the expression of *GJA4*, which encodes for the gap junction protein Cx37 (Connexin37). We found that expression of Cx37 is also downregulated by the inflammatory factor TNFα (tumor necrosis factor-α). In a mouse embryo model with disrupted SMAD1/5 signaling, loss of Cx37 from a localized vessel area correlates with development of a shunt directly connecting the dorsal aorta to the inlet of the heart. Mechanistically, loss of Cx37 did not affect proliferation nor did it cause EC hypertrophy, 2 proposed mechanisms that could result in vessel enlargement.[23,25] Loss of Cx37 did, however, result in altered directionality of EC migration under flow, which was also documented in a zebrafish model of AVM formation in response to *acvrl1* ablation and in mice lacking *Eng*, specifically in ECs.[21,26]

MATERIALS AND METHODS

The data that support the findings of this study are available from the corresponding author on reasonable request. For details of reagents used, please see the Major Resources Table and Materials and Methods in the online-only Data Supplement.

In Vitro Shear Stress

Human microvascular ECs (HMvEC)-Dermal were cultured in EGM-2MV medium or EC growth medium MV 2, with addition of penicillin/streptomycin. For all experiments, HMvECs were used at Passage 7. Knockdown of *GJA4* was performed using HiPerfect according to the manufacturer's directions. Knockdown of *SMAD1/5* was performed using Lipofectamine 2000 according to the manufacturer's

directions. HMvECs were grown to confluency on collagen I–coated (60 µg/mL) Superfrost Excell slides. For shear stress experiments, slides were washed 3× with PBS and placed in a custom-designed parallel plate flow chamber within a tissue culture incubator. Shear stress was applied using a peristaltic pump (Masterflex LS 7550-30) for laminar shear stress or a syringe pump (New Era Pump Systems NE-4000) for oscillatory shear stress. For static controls, slides were washed 3× with PBS, medium was subsequently refreshed, and cells were collected after an equivalent time period. All Western blots were performed using standard procedures, and uncropped blots are available in the online-only Data Supplement (Figure I in the online-only Data Supplement). For RNASeq, lysate from 4 separate slides was pooled for each replicate. Each slide was sheared independently in an individual chamber. RNA was extracted using RNEasy Kits (Qiagen) according to manufacturer's instructions. RNA sequencing was performed by the VIB Nucleomics Core (KU Leuven, Belgium). Detailed methods can be found in the online-only Data Supplement.

RNASeq Data Analysis

Low-quality ends and adapter sequences were trimmed off from the Illumina reads with FastX 0.0.14 and Cutadapt 1.7.1.[27,28] Subsequently, small reads (length <35 bp), polyA-reads (>90% of the bases equal A), ambiguous reads (containing N), low-quality reads (>50 % of the bases <Q25), and artifact reads (all but 3 bases in the read equal one base type) were filtered using FastX 0.0.14 and ShortRead 1.24.0.[29] With Bowtie2 2.2.4, reads that align to phix_illumina were identified and removed.[30] The preprocessed reads were aligned with STAR aligner v2.4.1d to the reference genome of *Homo sapiens* (GRCh38).[31] Default STAR aligner parameter settings were used, except for "–outSAMprimaryFlag OneBestScore –twopassMode Basic –alignIntronMin 50 –alignIntronMax 500000 –outSAMtype BAM SortedByCoordinate". Using Samtools 1.1, reads with a mapping quality smaller than 20 were removed from the alignments.[32] The number of reads in the alignments that overlap with gene features were counted with featureCounts 1.4.6.[33] Following parameters were chosen: -Q 0 -s 2 -t exon -g gene_id. Genes for which all samples had <1 count per million were removed. Raw counts were further corrected within samples for GC content and between samples using full quantile normalization, as implemented in the EDASeq package from Bioconductor.[34] With the EdgeR 3.8.6 package of Bioconductor, a negative binomial generalized linear model was fitted against the normalized counts.[35] Normalized counts were not used directly, but offsets were used. Differential expression was tested for with a generalized linear model likelihood ratio test, also implemented in the EdgeR package. The resulting *P* values were corrected for multiple testing with Benjamini-Hochberg to control the false discovery rate.[36]

Quantitative Polymerase Chain Reaction

Quantitative polymerase chain reaction (PCR) was performed using SYBR Green PCR master mix and Applied Biosystems QuantStudio3. Primers were designed in house and synthesized by IDT. Primers are listed in the online-only Data Supplement.

Migration Assay

Human umbilical vein ECs (HUVECs) were used at Passage 5. Fifteen percent of the cells were dyed with CellTracker Green CMFDA dye. HUVECs were seeded onto the fibronectin-coated (15 µg/mL) surface of a custom-designed flow chamber. HUVECs were transfected with siRNA against *GJA4* or scrambled control siRNA using HiPerfect Transfection Reagent. HUVECs were pretreated for 2 hours in 200 pg/mL BMP9 and then exposed to 0.1 Pa shear stress for 5 hours in complete media. Imaging was performed on a Zeiss LSM 700 confocal microscope. One image was taken every 30 minutes. Migration analysis (cell tracking) was done using Imaris software.

Mouse Models

All experiments were approved by the KU Leuven Animal Ethics Committee. All mice were group-housed under conventional conditions in 12-hour day and night cycle environment with ad libitum availability of normal laboratory diet (ssniff R/M-H normally; ssniff M-Z during breeding) and water. To conditionally inactivate *Smad1* and *Smad5* in ECs, $RCE^{fl/fl};Smad1^{fl/fl};Smad5^{fl/fl}$ females (CD1 background) were crossed with $Tie2Cre^{Tg/0};Smad1^{fl/+};Smad5^{fl/+}$ males (CD1 background).[15] To produce heterozygous inactivation, $RCE^{fl/fl};Smad1^{fl/fl};Smad5^{fl/fl}$ females (CD1 background) were crossed with $Tie2Cre^{Tg/0}$ males (CD1 background). Embryos were dissected between 8 and 9.5 days of gestation. Embryos were allocated randomly to groups such that each well had approximately the same average stage (embryos are cultured 3 per well). Genotype was tested after culturing and evaluation of vascular phenotype.

Embryo Culture

Dams were euthanized at embryonic day (E) 8.5, and embryos were cultured within their yolk sacs as previously described.[37] For cultures with TNFα, embryos were allowed to recover for 1 to 3 hours, depending on stage, before addition of compounds. Embryos were staged as follows: 0 to 2 somites E8.0; 2 to 4 somites E8.25; 5 to 8 somites E8.5; 8 to 11 somites E8.75; 12 to 15 somites E9.0; 15 to 18 somites E9.25; and 19 to 23 somites E9.5.

Blood Flow Analysis

Analysis of blood flow patterns was performed as previously described.[38] Using a pulled quartz needle and a pico-spritzer, embryos were injected intravascularly in the yolk sac with a single pulse of PEGylated FluoSpheres. The motion of the FluoSpheres was imaged at 125 frames per second for 2 entire cardiac cycles using a Photron Fastcam APX-rs camera. Blood velocity in the inlets and outlets of the vessels was calculated by microparticle image velocimetry analysis and combined with vessel geometry as the input for computational fluid dynamic analysis. For analysis of perfusion, a single pulse of TRITC-dextran was injected intravascularly. Only embryos with a strong heartbeat were analyzed.

Immunostaining

Yolk sacs were fixed in ice cold Dent's fixative overnight at –20°C. For Cx37 staining, tyramide amplification was used as

per manufacturer's instructions. The membrane specificity of Cx37 staining was verified at high magnification (Figure II in the online-only Data Supplement).

Quantification and Statistical Analysis

For analysis of quantitative PCR and Western Blot results and comparisons of *GJA4* knockdown cells to controls, an unpaired 2-tailed *t* test was used. For comparison of distributions of angles, a Kolmogorov-Smirnov test was used. For analysis of multiple comparisons, 2-way ANOVA followed by Sidak multiple comparison test was performed, as indicated in the figure captions. For analysis of vascular malformation count data, Fisher exact test was performed.

RESULTS

Cx37 (*GJA4*) Is a Specific Target of Shear Stress–Induced SMAD1/5/9 Signaling

Shear stress has been reported to induce phosphorylation of SMAD1/5/9 in ECs in vitro.[19,24] To determine the kinetics of SMAD1/5/9 phosphorylation, confluent HMvECs were exposed to 1.5 Pa shear stress for 0.5 to 4 hours. To prevent uncontrolled inclusion of BMPs in the medium, we replaced fetal bovine serum (FBS) in our medium with 15% synthetic knockout serum replacement (KOSR). Levels of total SMAD1/5/9 protein did not change with shear stress; however, we saw a maximum phosphorylation of SMAD1/5/9 at 0.5 hours, which declined with longer exposure times to shear stress (Figure 1A). To determine the intensity of shear stress inducing robust SMAD1/5/9 phosphorylation, we exposed ECs to a physiological range of shear stress intensities from 0.15 to 3.0 Pa for 0.5 hours. SMAD1/5/9 phosphorylation increased in a dose-response manner with increasing levels of shear stress and was comparable at 1.5 to 3 Pa to levels of p-SMAD1/5/9 (SMAD1/5/9 phosphorylation) induced by 200 pg/mL BMP9 (=17 pmol/L; Figure 1B).

KOSR was reported by the manufacturer to contain only albumin, insulin, and transferrin proteins. Though no BMPs are supplemented in KOSR, the lipid-rich albumin component (AlbuMAX) is purified from serum. Furthermore, BMPs are not the only known ligands of ALK1, as TFGβ[7] and LDL (low-density lipoprotein) have also been shown to directly bind the receptor.[39] To verify that 15% KOSR medium was free of all potential ALK1 ligands, we sheared ECs at 3.0 Pa or treated them with BMP9, with or without the addition of the soluble ligand scavenger ALK1-Fc.[40] We used medium with 1% BSA as a control containing the same total amount of albumin (Figure 1C). In the 1% BSA condition, BMP9 induced SMAD1/5/9 phosphorylation but shear stress did not induce SMAD1/5/9 phosphorylation. In the 15% KOSR condition, both shear stress and BMP9 induced SMAD1/5/9 phosphorylation, but the addition of 50 ng/mL ALK1-Fc (=1.3 μmol/L) prevented this in both conditions, indicating the presence of an ALK1 ligand in KOSR. We performed all further shear stress experiments using medium with 0.1% BSA to reduce distortion of Western blot bands by albumin. ALK1-Fc (50 ng/mL) was supplemented to this medium whenever we wished to prevent shear stress–induced SMAD1/5/9 phosphorylation.

It has previously been reported that shear stress amplifies SMAD1/5 phosphorylation in response to ligand.[19] To verify this, we sheared ECs with increasing concentrations of BMP9 from 0.1 to 100 pg/mL (0.08–8 pmol/L). We found that at low concentrations of BMP9, shear stress amplified SMAD1/5/9 phosphorylation compared with static conditions, while at higher BMP9 concentrations, shear stress only slightly augmented SMAD1/5/9 phosphorylation over the addition of BMP9 in the static condition (Figure 1D).

Although our results show that shear stress amplifies SMAD1/5/9 phosphorylation only in response to extremely low levels of ligand, even at higher BMP9 concentrations, the combination of transcription factors present in the nucleus under static and shear conditions will not be the same. Furthermore, levels of circulating BMP9 in blood plasma are much higher than the range where amplification occurs, though whether all circulating BMP9 is bioavailable is currently unknown. For these 2 reasons, we hypothesized that shear stress and BMP9 signaling may interact to regulate specific target genes, which BMP9 signaling alone does not affect. We performed an RNASeq analysis to identify targets modulated by shear stress–induced BMP9 signaling. HMvECs in 0.1% BSA media were exposed to 2 hours of either (1) static conditions in the presence of ALK1-Fc, (2) static conditions in the presence of high concentration BMP9 (200 pg/mL), (3) 3.0 Pa shear stress in the presence of ALK1-Fc, or (4) 3.0 Pa shear stress in the presence of low concentration BMP9 (1 pg/mL; Figure 1E). These conditions were chosen such that low BMP9 with shear stress induced comparable SMAD1/5/9 signaling to high BMP9 under static conditions (eg, see *ID1* expression in Figure IIID in the online-only Data Supplement). It should be noted that neither *BMP9* nor *BMP10* was expressed by ECs in our system (not shown, from RNASeq results), which agrees with reports that these proteins are expressed exclusively by the heart and liver, respectively, and delivered to ECs through the circulating blood.[41,42]

Among 58 234 unique targets assessed by RNA-Seq analysis, 61 transcripts were identified that were at least 2-fold significantly ($P<0.05$) up- or downregulated compared with the static with ALK1-Fc condition only in the shear stress with low BMP9 condition but were not in either the static with high BMP9 or the shear stress with ALK1-Fc conditions (Figure 1F). Of the 61 genes, we focused on genes known to be important for arteriovenous identity, specifically *GJA4*, *SEMA3G*, and

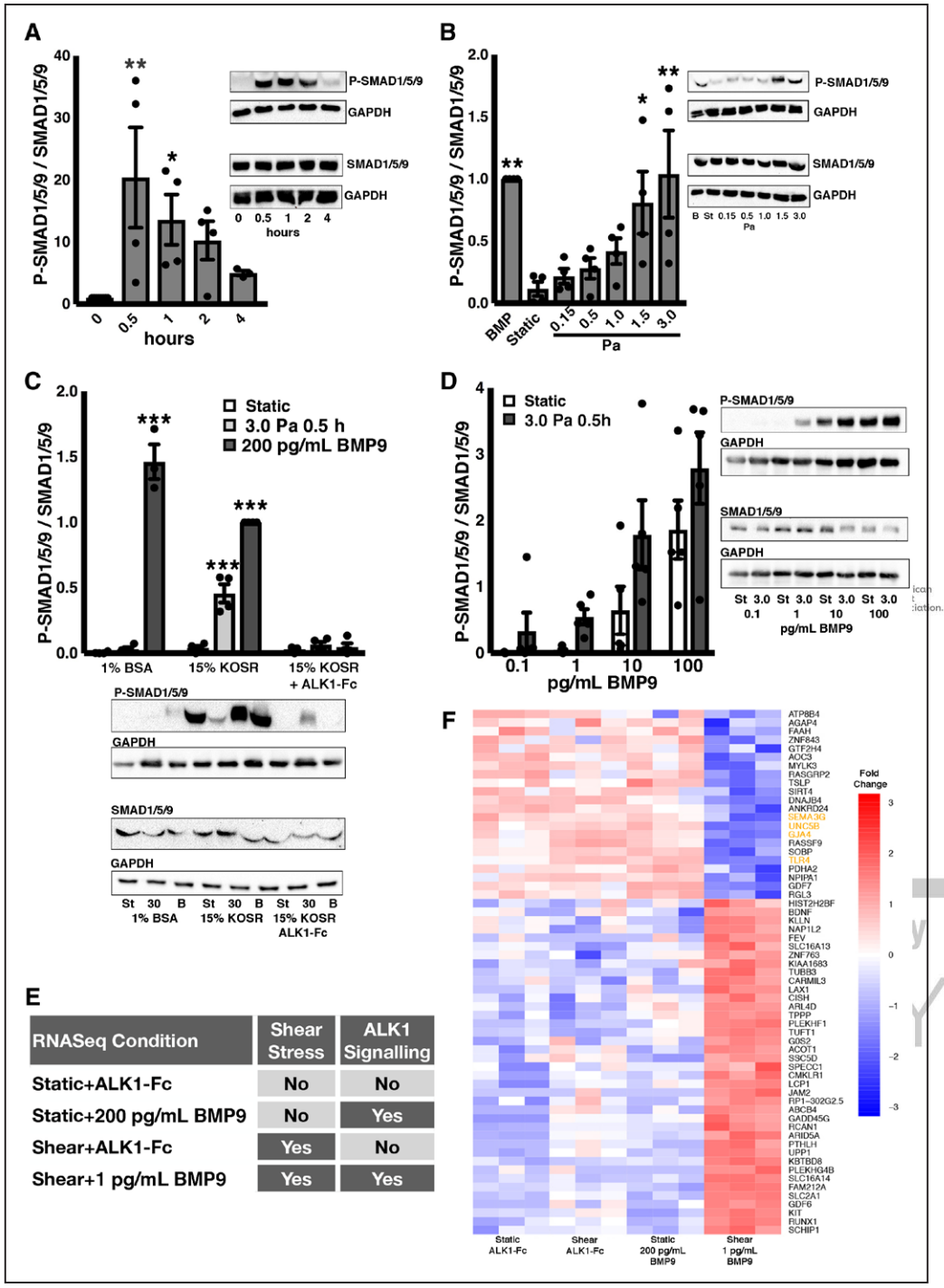

RNASeq Condition	Shear Stress	ALK1 Signalling
Static+ALK1-Fc	No	No
Static+200 pg/mL BMP9	No	Yes
Shear+ALK1-Fc	Yes	No
Shear+1 pg/mL BMP9	Yes	Yes

Figure 1. Shear stress induces SMAD1/5/9 phosphorylation in a ligand-dependent manner.
A, Densitometry and representative Western blots of p-SMAD1/5/9 levels relative to total SMAD1/5/9 protein (≈60 kDa) in human microvascular endothelial cells (HMvECs) exposed to 1.5 Pa shear stress for different times. **B**, Densitometry and representative Western blots for p-SMAD1/5/9 levels relative to total SMAD1/5/9 protein in HMvECs exposed to different levels of shear stress for 0.5 h. Data were normalized to p-SMAD1/5/9 levels that occurs when ECs (endothelial cells) are exposed to 200 pg/mL BMP9 (bone morphogenetic protein) for 0.5 h under static conditions, indicated as BMP. **C**, Densitometry and representative Western blots for p-SMAD1/5/9 levels relative to SMAD1/5/9 protein in HMvECs exposed for 0.5 h to 3.0 Pa shear stress or 200 pg/mL BMP9 in the presence of medium containing 1% BSA or 15% knockout serum replacement (KOSR), with or without the addition of the scavenging receptor ALK1-Fc (50 ng/mL). (*Continued*)
D, Densitometry and representative Western blots of p-SMAD1/5/9 levels relative to total SMAD1/5/9 protein in HMvECs exposed for 0.5 h to 3.0 Pa shear stress in medium containing 0.1% BSA with increasing concentrations of BMP9. **E**, Experimental design for RNASeq experiment. **F**, Heatmap of 61 candidate genes of interest from RNASeq. GAPDH (≈35 kDa) was used as a loading control for all Western blots. n=3–4 per condition for all panels. Error bars represent SEM. Significance relative to static condition 2-way ANOVA followed by Sidak multiple comparison test (A–D). *P<0.05, **P<0.01, and ***P<0.001. For full Western blots, see Figure I in the online-only Data Supplement.

UNC5B (Figure 1F, orange text). We also selected *TLR4* (Figure 1F, orange text) because its activation triggers cerebral cavernous malformations, another vascular malformation.[43] We performed quantitative PCR to verify the RNASeq results (Figure 2A; Figure IIIA through IIIC in the online-only Data Supplement). *GJA4*, *SEMA3G*, *UNC5B*, and *TLR4* all showed a BMP9- and shear stress–specific pattern of regulation. Their expression was induced by application of BMP9 in static conditions, but this effect was inhibited in the presence of a combination of BMP9 and shear stress (Figure 2A; Figure IIIA through IIIC in the online-only Data Supplement). In the absence of ALK1 ligand (ALK1-Fc conditions), shear stress had no effect on these genes.

The gene that showed the strongest upregulation was *GJA4* (encoding for Cx37). Cx37 is a vascular gap junction protein important for restricting EC proliferation,[44,45] and mice lacking Cx37 have increased blood vessel diameters as well as increased numbers of collateral vessels.[46,47] Gap junctions have also been suggested to be necessary for preventing vascular shunt formation, based on in silico models.[48] Since excess EC proliferation and expansion of vessel diameter are key features of AVM formation, we proceeded to further investigate the involvement of Cx37 in AVM formation.

SMAD1/5-Dependent and Independent Signaling Differentially Regulate GJA4 (Cx37) Expression Downstream of BMP9

While our results showed that shear stress prevented *GJA4* expression after 2 hours of BMP9 treatment, it is generally accepted that laminar shear stress increases endothelial *GJA4* expression in vitro (eg,, Pfenniger et al[49] and ECs in large arteries express Cx37 in vivo[49–51]). Oscillatory shear stress has been similarly shown to induce Cx37 expression in lymphatic ECs; Cx37 is expressed by ECs on the downstream side of lymphatic valves, where it is induced by oscillatory lymphatic flow.[52,53] To better understand the apparent contradiction between published results and our own data, we generated a more complete series of experiments to investigate Cx37 regulation under different hemodynamic conditions.

We exposed ECs to shear stress in the absence of BMP9 and under low and high BMP9 conditions. In agreement with our RNASeq samples, high BMP9 induced a marked increase in Cx37 expression in static conditions, but this effect was repressed under shear stress (Figure 2A). *KLF2* expression was increased in all shear stress conditions (Figure IIID in the online-only Data Supplement), indicating that other aspects of mechanotransduction occurred normally. Likewise, a classical target of phosphorylated SMAD1/5/9, *ID1*, was strongly expressed in the presence of high BMP9 in both shear stress and static conditions and in the presence of low BMP9 when concurrently exposed to shear stress (Figure IIID in the online-only Data Supplement). ALK1-Fc repressed all activation of *ID1* (Figure IIID in the online-only Data Supplement). This pattern of *ID1* expression is in agreement with our results showing that shear stress is required for SMAD1/5/9 phosphorylation in low BMP9 conditions (Figure 1D) and that SMAD1/5/9 phosphorylation is effectively repressed by ALK1-Fc (Figure 1C).

To determine whether the suppression of BMP9-induced Cx37 expression by shear stress was specific to higher levels of shear stress, we also tested the effect of lower levels of laminar shear stress and oscillatory shear stress. Similar to the higher shear stress results, both 0.5 Pa laminar shear stress and ± 0.5 Pa oscillatory shear stress did not affect Cx37 expression alone, and both could repress Cx37 expression that was induced by BMP9 (*GJA4*; Figure 2B and 2C). Under both low laminar and oscillatory shear stress, *KLF2* expression was activated by shear stress and *ID1* expression was activated when BMP9 was present (Figure IIIE through IIIF in the online-only Data Supplement).

Previous reports of shear stress–induced Cx37 upregulation used ECs exposed to shear stress for longer times and in the presence of FBS.[49] We therefore performed 24-hour shear stress experiments with complete medium containing 5% FBS. In agreement with previous reports, we found that under these conditions, Cx37 expression was upregulated under shear stress (Figure 2D). As anticipated, given the high levels of BMP9 and BMP10 found in serum, *ID1* was strongly activated in the complete medium condition, and this was further enhanced by 24 hours of shear stress (Figure IIIG in the online-only Data Supplement). Since Notch signaling is known to co-regulate Cx37 expression, we attempted to scavenge any soluble Notch ligands in FBS using Notch-Fc; however, addition of Notch-Fc to the media did not alter the shear stress–induced expression of Cx37 in complete media (Figure 2D). However, when ALK1 ligands were chelated from the complete media using ALK1-Fc, Cx37 upregulation by shear stress was prevented, indicating that an ALK1 ligand allowed for upregulation of Cx37 when FBS is included in the media (Figure 2D).

To identify which ALK1 ligand was involved, we exposed ECs to shear stress in media containing 0.1% BSA and various known ALK1 ligands (Figure 2E). For BMP9 and LDL, ligand treatment upregulated Cx37 under static conditions, but this effect was repressed by shear stress. TGFβ failed to upregulate Cx37 expression under static conditions and even baseline Cx37 was reduced under shear stress. BMP10, however, induced Cx37 expression under static conditions, and expression of Cx37 was amplified by 24 hours of shear stress, indicating that BMP10 may be responsible for the upregulation of Cx37 that is observed under high shear stress with media containing FBS, as well as in the adult aorta.[49]

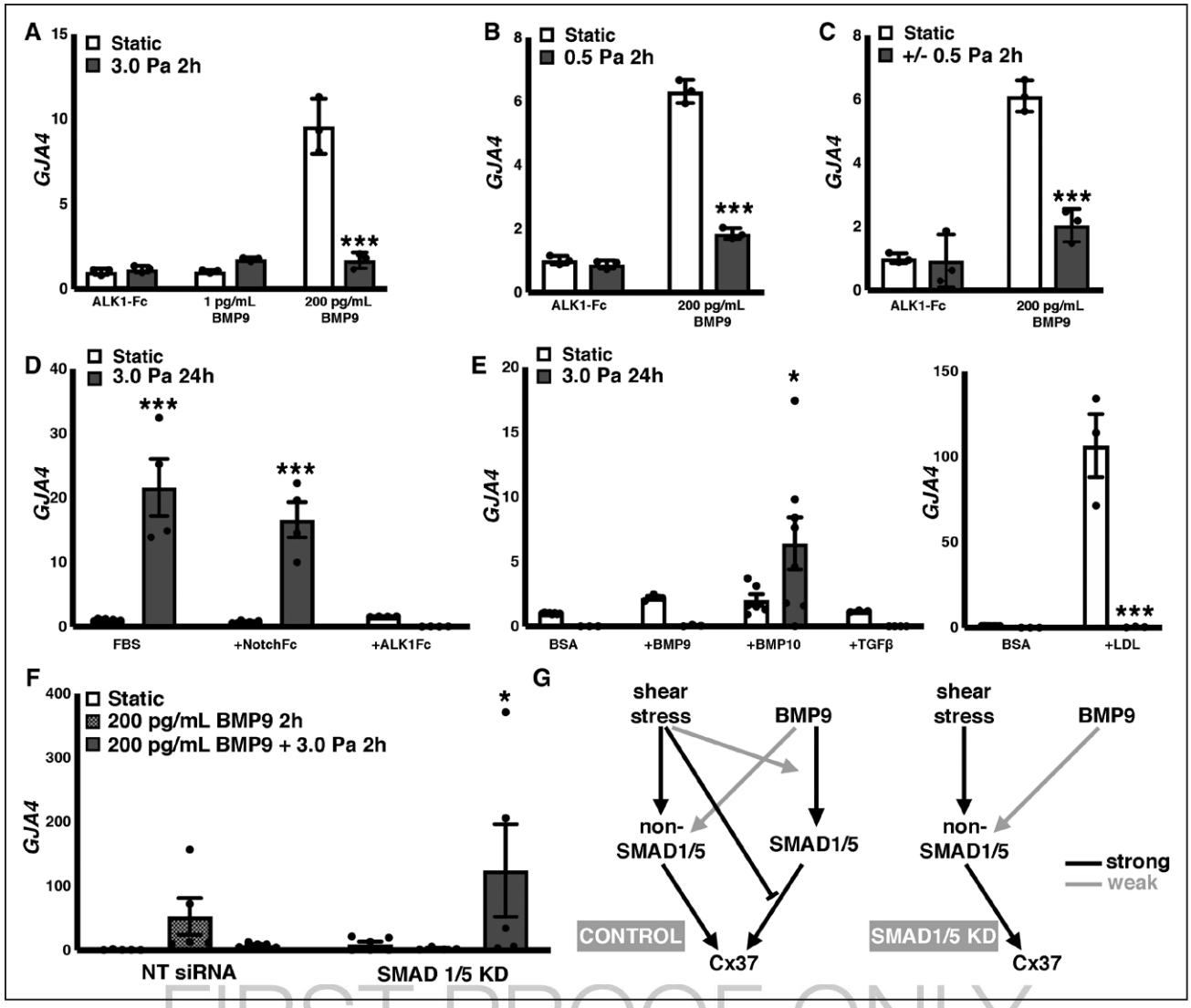

Figure 2. BMP9-induced GJA4 (Cx37 [Connexin 37]) expression is inhibited by shear stress.
A, Expression of GJA4 mRNA by human microvascular endothelial cells (HmvECs) following exposure to 2 h of 3.0 Pa shear stress in the presence of 50 ng/mL ALK1-Fc, or 1 or 200 pg/mL BMP9 (bone morphogenetic protein). n=3–4 per condition. **B**, Expression of GJA4 mRNA by HMvECs following exposure to 2 h of 0.5 Pa shear stress in the presence of 50 ng/mL ALK1-Fc or 200 pg/mL BMP9. n=3–4 per condition. **C**, Expression of GJA4 mRNA by HMvECs following exposure to 2 h of ±0.5 Pa oscillatory shear stress in the presence of 50 ng/mL ALK1-Fc or 200 pg/mL BMP9. n=3–4 per condition. **D**, Expression of GJA4 mRNA by HMvECs following exposure to 24 h of 3.0 Pa shear stress in the presence of 5% fetal bovine serum (FBS) with the addition of either 50 ng/mL Notch-Fc or 50 ng/mL ALK1-Fc. n=3–4 per condition. **E**, Expression of GJA4 mRNA by HMvECs following exposure to 24 h of 3.0 Pa shear stress in 0.1% BSA media with the addition of 200 pg/mL BMP9, BMP10, or TGFβ1. n=3–4 per condition. Expression of GJA4 mRNA by HMvECs following exposure to 24 h of 3.0 Pa shear stress in 0.1% BSA media with the addition of 5 μg/mL LDL (low-density lipoprotein). n=3 per condition. **F**, Expression of GJA4 mRNA by HMvECs transfected with nontargeting siRNA or siRNA against SMAD1 and SMAD5 in 0.1% BSA media with or without the addition of 200 pg/mL BMP9 and exposed to static condition or 3.0 Pa shear stress. n=5–6 per condition. **G**, Schematic of proposed SMAD1/5 and non-SMAD1/5 signaling induced by BMP and shear stress. Error bars represent SEM. Significance relative to static condition by 2-way ANOVA followed by Sidak multiple comparison test. $^{**}P<0.01$ and $^{***}P<0.001$. Extended quantitative polymerase chain reaction analysis available in Figure III in the online-only Data Supplement.

Since Cx37 expression did not mirror *ID1* or *KLF2* expression, we wondered whether noncanonical ALK1 signaling might be involved in the regulation of Cx37. We transfected HMvECs with nontargeting siRNA or *SMAD1/5* siRNA (Figure IIIH in the online-only Data Supplement) and exposed the cells to BMP9 under static conditions or laminar shear stress. When *SMAD1/5* were knocked down, BMP9 was unable to induce Cx37 expression under static conditions, indicating that Cx37 is downstream of SMAD1/5 signaling (Figure 2F). Curiously, shear stress actually upregulated Cx37 in the presence of BMP9 after knockdown of SMAD1/5. We propose that BMP9, as well as TGFβ and LDL, normally weakly activate non-SMAD1/5 pathways, but that in the

absence of SMAD1/5, the non-SMAD1/5 pathways are the prevalent signaling pathway (Figure 2G).

Formation of Vascular Shunts Occurs Spontaneously in Yolk Sacs of Endothelial-Specific *Smad1/5* Knockout Embryos

Loss of different extracellular receptors and intracellular effectors of the ALK1 signaling pathway, including ALK1, Endoglin, BMP9, and SMAD4, all result in AVM formation.[2–5] SMAD1/5/9 are the predominant effectors of this pathway, and therefore it was surprising that no AVMs have been reported for mice with mutations in these genes. We hypothesized that AVM formation may be transient in these mice. SMAD1 and SMAD5 are the predominant downstream effectors of ALK1/Endoglin signaling during development, while SMAD9 is dispensable.[13,15] We therefore investigated AVM development in mice with an EC-specific deletion of *Smad1* and *Smad5*. The EC-specific compound homozygous null embryos (*Tie2:Cre; Smad1*$^{fl/fl}$*; Smad5*$^{fl/fl}$) die at mid-gestation, whereas EC-specific compound heterozygous mice (*Tie2:Cre; Smad1*$^{fl/+}$*; Smad5*$^{fl/+}$) are viable and fertile.[15]

Yolk sac vasculature undergoes a profound process of flow-dependent vascular remodeling from E8.5 to E10.5.[54] We dissected embryos at an intermediate stage of remodeling: 15–18 somites as well as embryos at 22–25 somites, the stage at which we have previously observed defects in sprouting angiogenesis and a failure of vascular remodeling.[15] *Cre*-negative control embryos and endothelial-specific *Smad1* and *Smad5* heterozygous embryos (dHet^{EC} [mice with endothelial-specific heterozygous deletion of SMAD1/5]; *Cre*$^{+}$*;Smad1*$^{fl/+}$*;Smad5*$^{fl/+}$) developed normal, hierarchically organized yolk sac vasculature (Figure 3A and 3B). In embryos missing all 4 alleles of *Smad1* and *Smad5* in ECs (dKO^{EC} [mice with endothelial-specific deletion of SMAD1/5]; *Cre*$^{+}$*;Smad1*$^{fl/fl}$*;Smad5*$^{fl/fl}$), shunts that directly connect the heart and dorsal aorta were found in 2 out of 3 yolk sacs at 15–18 somites (Figure 3A). The vasculature of the third yolk sac consisted of a completely unremodeled capillary plexus. By 22–25 somites, the vasculature of dKO^{EC} yolk sacs resembled an unremodeled capillary plexus in all embryos (3 of 3 yolk sacs). Curiously, the presence of a previously existing shunt was evident when staining for αSMA (α-smooth muscle actin) was performed (Figure 3B), indicating that the vasculature had collapsed back to a plexus after first developing an AVM-like defect, rather than never remodeling in the first place.

TNFα Disrupts Cx37 Expression and Promotes Shunts in Vasculature With Disrupted SMAD1/5 Mechanotransduction

Gja4 (Cx37) is one of the first arterial genes expressed in development, occurring before the onset of flow and before the expression of any NOTCH receptors, BMP9, or BMP10.[55] Because other factors can regulate Cx37,[49,56] impaired SMAD1/5 signaling does not necessarily mean that Cx37 is completely absent in vessels. We therefore reasoned that other stimuli might function locally to further disrupt Cx37 expression and thereby permit vascular malformations. Inflammation and wounding have been proposed as possible local factors inducing AVM formation in HHT, as well as in the development of other vascular pathologies like cerebral cavernous malformation.[43,57,58] Wounding downregulates Cx37 expression in migrating ECs in vitro,[59] and TNFα has been reported to decrease Cx37 expression.[60] We pretreated ECs for 4 hours with high BMP9 and then exposed the cells to low concentration (0.5 nmol/L) TNFα in the presence of high BMP9 for 16 hours under static conditions. We found that TNFα abolishes BMP9-induced Cx37 expression in ECs in vitro (*GJA4*, Figure 4A). We verified that TNFα treatment did not disrupt ligand- or shear stress–induced SMAD1/5/9 phosphorylation (Figure IV in the online-only Data Supplement).

To investigate the role of Cx37 in the development of vascular malformations in vivo, we used the developing mouse embryonic yolk sac vasculature as a model. We treated E8.5 *Cre*-negative, dHet^{EC}, or dKO^{EC} embryos with TNFα in culture for 24 hours. None of the *Cre*-negative embryos was identified as having a shunt (Figure 4B). In the presence of TNFα, however, over half of dHet^{EC} embryos formed vascular malformations with a direct connection between the dorsal aorta to the inlet of the heart that were readily visible in the intact yolk sac under white light (black arrowheads, Figure 4C; Figure V in the online-only Data Supplement). dKO^{EC} embryos developed highly chaotic yolk sac vasculature, with massive shunts and enlarged vascular sinuses (Figure 4D), which made accurate quantification of AVM-like shunts impossible. The yolk sac vascular phenotype was confirmed by VE-Cadherin staining. The presence of vascular defects was scored in white light by a blinded observer (Figure 4E). The strong induction of AVM-like defects by TNFα in the dHet^{EC} embryonic yolk sacs supports the idea that downregulation of Cx37 in vasculature with impaired SMAD1/5 mechanotransduction contributes to AVM pathogenesis.

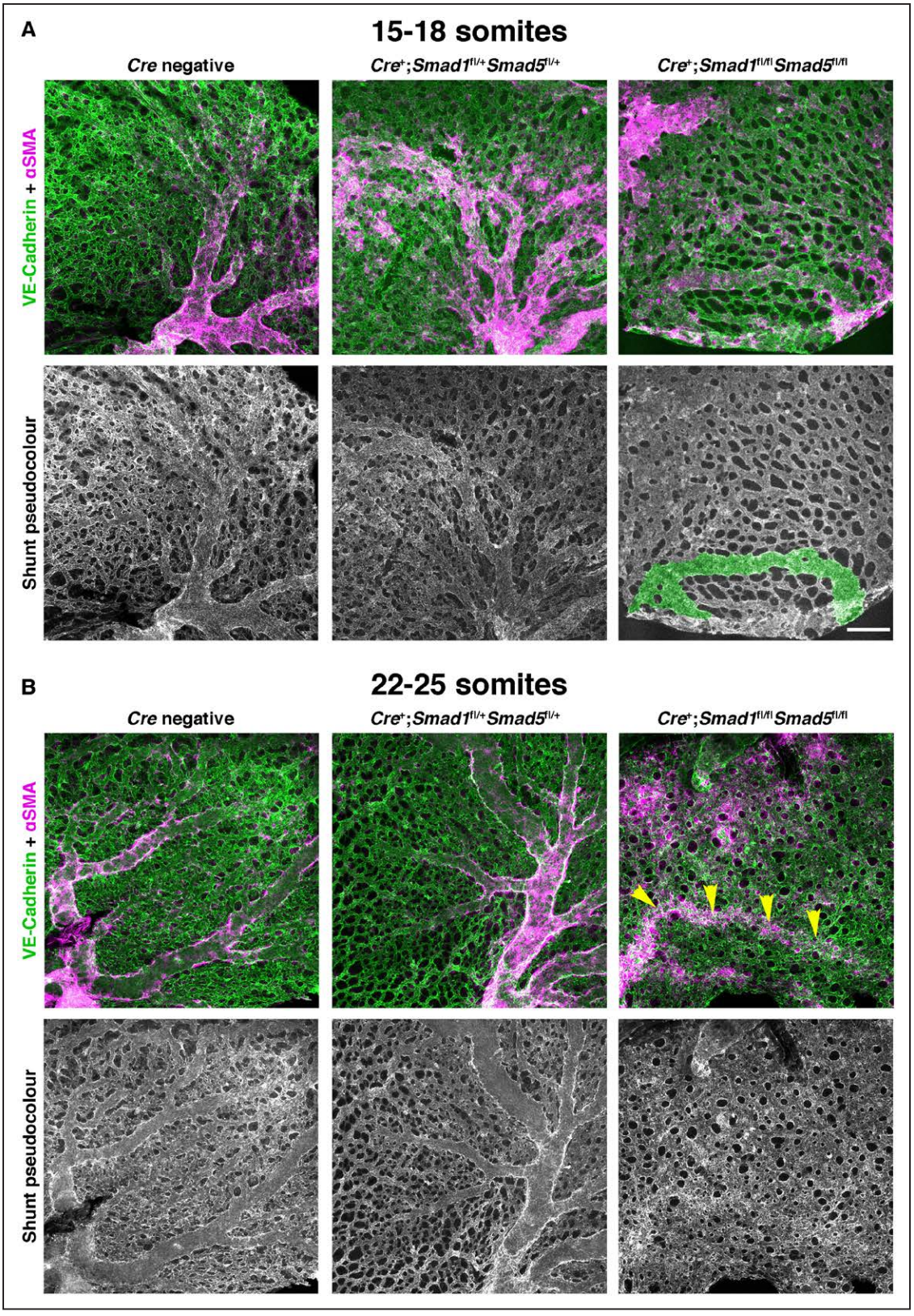

Figure 3. Smad1/5 double knockout embryos spontaneously form vascular shunts at E9.25.
Representative images of freshly isolated Cre negative, Cre^{+};$Smad1^{fl/+}$;$Smad5^{fl/+}$ ($dHet^{EC}$ [mice with endothelial-specific heterozygous deletion of SMAD1/5]), and Cre^{+};$Smad1^{fl/fl}$;$Smad5^{fl/fl}$ (dKO^{EC} [mice with endothelial-specific deletion of SMAD1/5]) yolk sacs at (**A**) E9.25 and (**B**) E9.5 stained for VE-Cadherin (green) and αSMA (α-smooth muscle actin; magenta), with shunts pseudocolored in green. Yellow arrowheads: αSMA staining indicating the location of a collapsed AVM-like shunt. Scale bar=200 μm, n=3 per genotype for each stage.

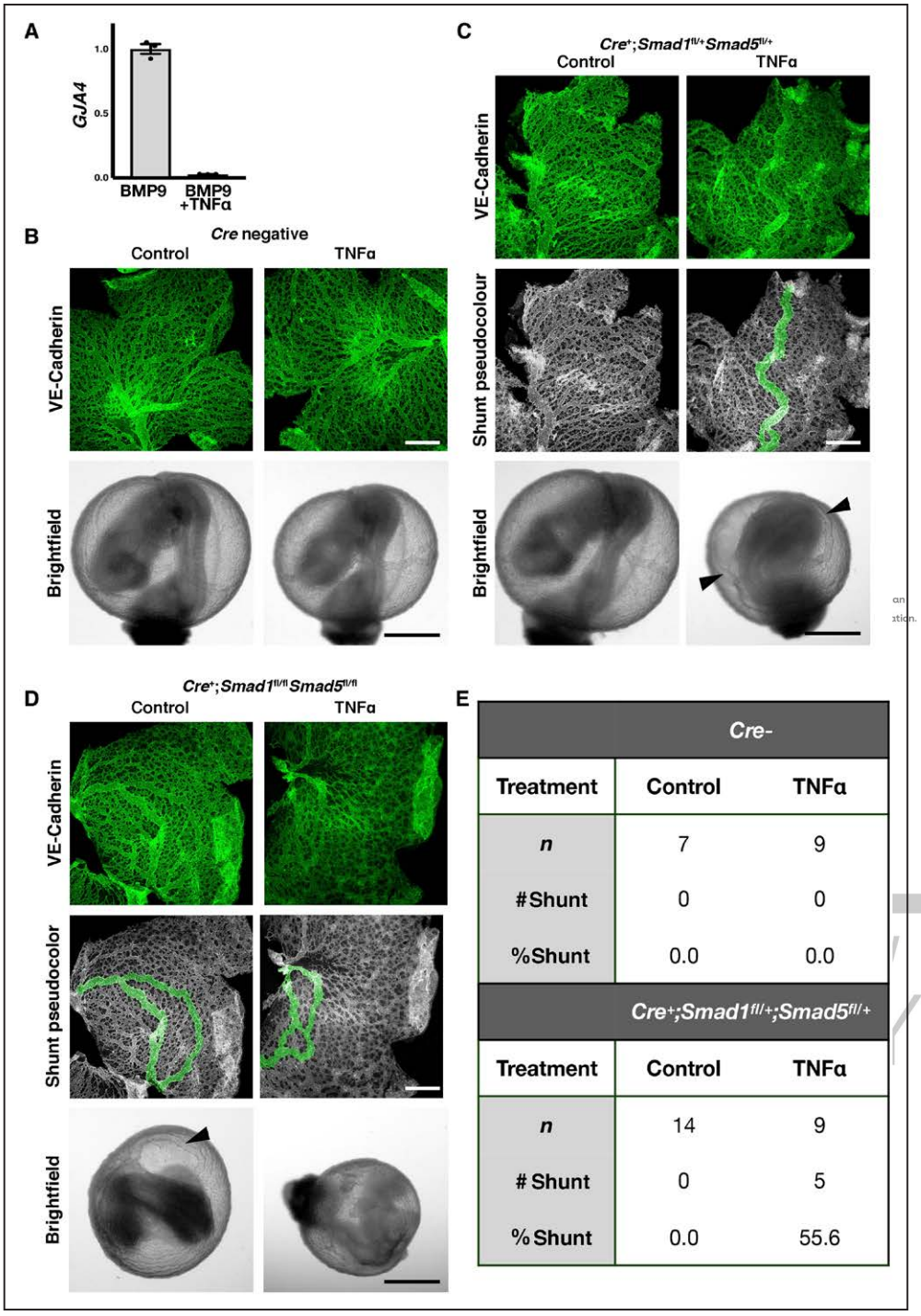

E

Cre-		
Treatment	Control	TNFα
n	7	9
#Shunt	0	0
%Shunt	0.0	0.0
Cre+;Smad1fl/+;Smad5fl/+		
Treatment	Control	TNFα
n	14	9
# Shunt	0	5
% Shunt	0.0	55.6

Figure 4. TNFα abolishes GJA4 (Cx37 [Connexin 37]) expression and induces formation of vascular shunts in a model of disrupted ALK1 signalling.

A, Expression of GJA4 mRNA by human microvascular endothelial cell (HMvECs) following exposure to 200 pg/mL BMP9 (bone morphogenetic protein) for 4 h and subsequent 16-hour exposure to 200 pg/mL with or without 0.5 nmol/L TNFα. n=3 per condition. Error bars represent SEM. Two-tailed unpaired *t* test. ***$P<0.01$. Representative images of yolk sacs from (**B**) Cre negative, (*Continued*) (**C**) Cre^{+};$Smad1^{fl/+}$;$Smad5^{fl/+}$ ($dHet^{EC}$ [mice with endothelial-specific heterozygous deletion of SMAD1/5]), and (**D**) Cre^{+};$Smad1^{fl/fl}$;$Smad5^{fl/fl}$ (dKO^{EC} [mice with endothelial-specific deletion of SMAD1/5]) E8.5 embryos treated with 0.5 nmol/L TNFα or control for 24 h and stained for VE-Cadherin, with shunts pseudocolored in green. Scale bar=500 μm. Bright field images of embryos after 24 h of culture. Scale bar=1 mm. Black arrowheads indicate shunts. **E**, Presence of shunts in yolk sacs from E8.5 mouse embryos treated for 24 h with 0.5 nmol/L TNFα or control, as scored by a blinded observer. # shunts indicates the total number of yolk sacs exhibiting at least one vascular defect connecting the dorsal aorta and the inlet to the heart. % shunts indicates the percent of yolk sacs exhibiting at least one shunt. Fisher exact test $P=0.00022$.

Flow Is Limited to Embryonic Vascular Shunts Which are Covered Over the Entire Length by Smooth Muscle Cells

The large shunts that we observed in the yolk sac connected the outflow from the dorsal aorta directly to the inlet of the heart, without perfusing any intermediate capillary vessels (Figure V in the online-only Data Supplement). We therefore quantified the flow within the arteriovenous shunts of dHet^{EC} embryos cultured overnight in TNFα or control embryos. PEGylated fluorescent microspheres were injected into the vasculature, and high-speed video recordings (125 fps) were made to visualize the flow patterns (Movies I and II in the online-only Data Supplement). These movies were quantified using microparticle image velocimetry. In control embryos, we observed a distribution of flow from higher flow vessels to progressively lower flow in surrounding branches (Figure 5A). In contrast, in yolk sacs with AVM-like defects, almost no flow was present outside the shunt and only the large vessel was well perfused (Figure 5B). We selected an area of interest from each vascular bed (white box) and performed computational fluid dynamic analysis on the vessel segments.[38] In control embryos, blood velocities in the large vessel reached levels of 1000 μm/s, with a gradual drop to lower velocities as the vessels branched out (Figure 5A). In contrast, shunts contained flow velocities of 800 μm/s, but this flow did not distribute through branching vessels (Figure 5B).

To verify our observation from computational fluid dynamic analysis that blood flow was largely limited to the loop of vessels connecting the dorsal aorta to the inlet of the heart, Cre-negative and dHet^{EC} embryos were cultured overnight in TNFα. Embryos were intravascularly injected with fluorescent dextran, and perfusion was visualized for 4 minutes (Figure 5C and 5D). Dextran-injection location is indicated by the magenta arrow. Injection creates a hotspot and labels an area of the vasculature, not a single vessel. In *Cre*-negative embryos, dextran was rapidly perfused throughout the entire vascular system and by 4 minutes vessels were evenly filled with dextran (Figure 5C). In contrast, in dHet^{EC} embryos with shunts, dextran was not distributed into systemic circulation, even after 4 minutes (Figure 5D). Some diffusion of the dextran was observed at later time points, resulting in labeling of surrounding capillaries (yellow arrowheads). The confinement of diffusion to the other vessels and not to avascular regions of the tissue also confirms that the dextran remains in the blood vessels and does not leach out in the time scale observed. It should be noted that dHet^{EC} embryos that did not develop vascular malformations showed normal perfusion, comparable to *Cre*-negative embryos.

In the dKO^{EC} embryos at E9.25, we had observed that the shunts were covered with smooth muscle cells for their entire length. In the control embryos, both the main artery and branches off of it expressed αSMA (Figure 5E), while vascular malformations of TNFα treated heterozygous embryos were surrounded by smooth muscle cells over the entire length without branching (Figure 5F).

Cx37 Expression Is Absent in Regions Where Vessels Are Enlarging

We next examined the spatiotemporal localization pattern of Cx37 during normal development and in our model of vascular malformation. We found that in the embryonic yolk sac, Cx37 is ubiquitously present in the vasculature before the onset of flow (Figure 6A; E8.5). Some regions lacking Cx37 expression are present in the blood islands (cyan arrowheads, Figure 6A). Surprisingly, we found that in early phases of vascular remodeling (E8.75), Cx37 is strongly expressed in the capillaries but is completely absent from areas where vessels are enlarging (Figure 6B). Since Cx37 expression in the vessels proceeds onset of BMP9 expression. BMP10 mRNA expression is only detected by in situ hybridization beginning at E9.5.[42] BMP10 mRNA has been detected as early as E8.75 by reverse transcriptase PCR/quantitative PCR of whole embryos.[41,61] It is unclear when protein would therefore be present at levels high enough to signal, but this is not likely to occur earlier than E9.0, so is also not likely to be driving early Cx37 expression. Its expression must be driven by either another ALK1 ligand (ie, LDL or TGFβ) or else another signaling pathway active during early vascular development (eg, Notch). At later phases of development (E9.5), Cx37 expression becomes restricted to arteries, as previously reported for adult mice[62] (Figure 6C, see also inset). This suggests that Cx37 is not an "arterial" marker per se, but rather that it is present in stable vessels where the diameter is not changing, and that it is downregulated to permit enlargement. This observation is in agreement with the work of Fang et al[56] showing that Cx37 promotes EC quiescence, which, in mature vasculature, would indeed correspond to a mature arterial phenotype, but in the early embryonic yolk sac, vasculature would correspond to the nonremodeling areas of the capillary plexus.

To examine the role of SMAD1/5 in the regulation of Cx37 expression, we compared *Cre*-negative and dKO^{EC} yolk sacs collected at E9.5. While *Cre*-negative yolk sacs expressed Cx37 largely in the arteries, there was very little Cx37 expression in dKO^{EC} yolk sacs, with erratic patches of Cx37 expression (Figure 6D). To verify how Cx37 expression related to defective vessel enlargement formation in our models, we cultured embryos for 10 hours, rather than overnight, to investigate Cx37 expression as vessels were enlarging, before vascular defects were present. *Cre*-negative embryos and control cultured dHet^{EC} embryos expressed Cx37 in the same pattern as E8.75 embryos: Cx37 was strongly expressed in the

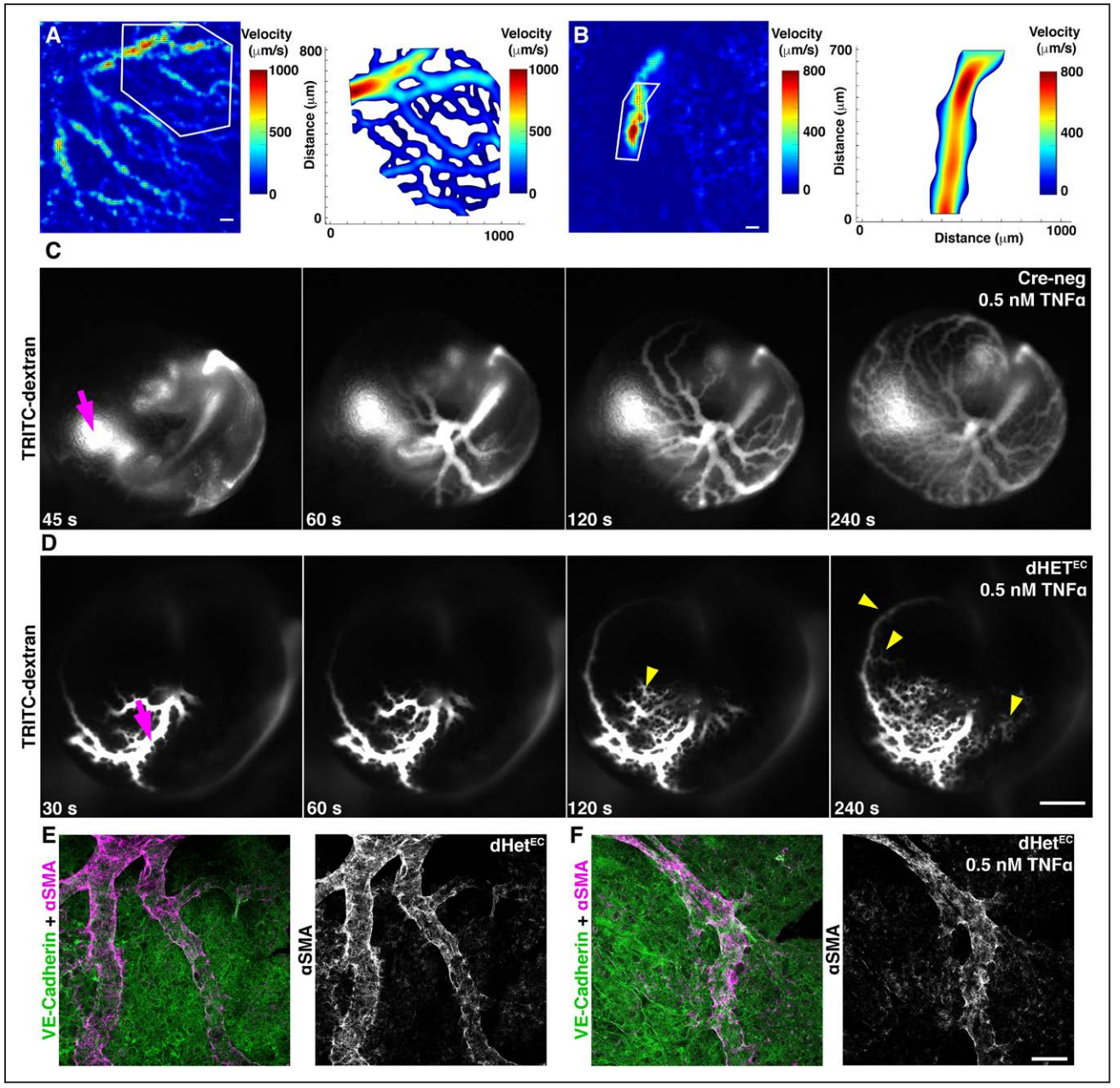

Figure 5. Vascular defects display characteristics of an arteriovenous malformation (AVM), with flow bypassing the capillary bed. Velocities of blood flow in yolk sac vasculature of control (**A**) and TNFα treated (**B**) dHet^{EC} (mice with endothelial-specific heterozygous deletion of SMAD1/5) embryos, obtained from microparticle image velocimetry (μPIV). White box indicates area of interest for computational fluid dynamics analysis of the blood flow in control and TNFα treated embryos. Cre-negative (Cre-neg; **C**) and dHET^{EC}; **D**) embryos were cultured overnight in the presence of TNFα and subsequently intravascularly injected with TRITC-dextran. Magenta arrow indicates site of injection. Distribution of dextran was followed for 4 min. Yellow arrowheads indicate areas of passive diffusion of dextran within the vasculature. α-Smooth muscle actin staining of control vasculature (**E**) and an AVM-like structure (**F**). Scale bar=100 μm (**A** and **B**). Scale bar=500 μm (**C** and **D**). Scale bar=200 μm (**E** and **F**). Movies of FluoSpheres are available in Movies S1 and S2 in the online-only Data Supplement. αSMA indicates α-smooth muscle actin.

capillaries and absent where larger vessels were forming (Figure 6E through 6G). The addition of TNFα to the medium of dHet^{EC} embryos consistently disrupted this expression pattern, resulting in Cx37-negative patches within the capillary plexus (3 of 3 yolk sacs; yellow arrowheads, Figure 6H).

Cx37 Is Necessary for Upstream Migration Under Flow

Since Cx37 is described as an arterial marker,[62] we first questioned whether Cx37 contributes to arterial and venous segregation. We tested whether ECs expressing high or low levels of Cx37 would self-segregate from

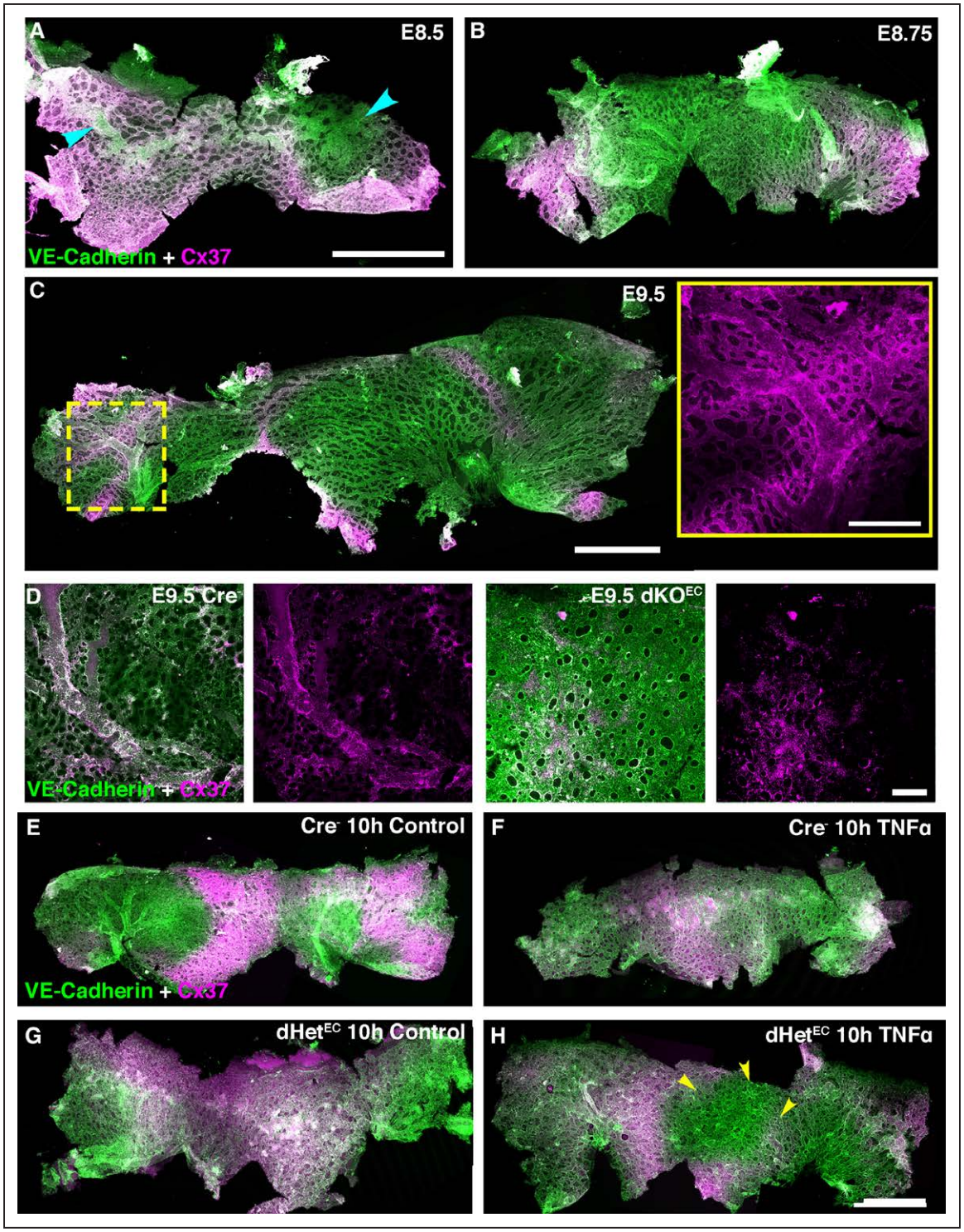

Figure 6. Cx37 (Connexin 37) localization initially correlates to nonenlarging capillary vessels but later becomes more restricted to arteries.

Cx37 expression in yolk sac vasculature at (**A**) E8.5, (**B**) E8.75, and (**C**) E9.5. Cyan arrowheads indicate blood islands at E8.5. **C** (Inset), Higher magnification image showing only Cx37 staining of the arterial region highlighted with the dotted lines. **D**, Cx37 expression in E9.5 Cre-negative and dKO^{EC} [mice with endothelial-specific deletion of SMAD1/5] yolk sacs. **E**–**H**, Cx37 expression in yolk sac vasculature of E8.5 Cre-negative and dHet^{EC} (mice with endothelial-specific heterozygous deletion of SMAD1/5) embryos cultured for 10 h with and without 0.5 nmol/L TNFα. Yellow arrowheads indicate patches of disrupted Cx37 expression. VE-cadherin (green) and Cx37 (magenta). All panels were produced by stitching together multiple images taken with a 5× objective lens, using Adobe Photoshop's photomerge function. n=3–4 per condition. Scale bar, **A**=1 mm. Scale bar, **B**–**C**=1 mm. Scale bar inset, **C**=300 µm. Scale bar, **D**=200 µm. Scale bar, **E**–**H**=1 mm. For higher magnification images of Cx37 staining, see Figure II in the online-only Data Supplement.

each other based on intercellular communication, in a similar manner to self-segregation based on differential expression of adhesion molecules (eg, Foty et al[63]). We mixed CellTracker Red-labeled, Cx37-knocked down ECs with ECs treated with scrambled siRNA, under high BMP9 conditions. For controls, all ECs were treated with scrambled siRNA (Figure VIA in the online-only Data Supplement). We verified that the Cx37 siRNA repressed BMP9-induced Cx37 expression (Figure VIB in the online-only Data Supplement) using an antibody developed by Simon et al.[64] We found no difference in the surface area of clusters of labeled cells between control and experimental conditions (Figure VIA and VIC in the online-only Data Supplement).

We then investigated whether Cx37 could be driving expression of arteriovenous identity markers. We transfected HMvECs with scrambled siRNA or siRNA targeting *GJA4* and subsequently treated the cells with BMP9 for 2 hours (Figure VIIA in the online-only Data Supplement). BMP9 induced expression of *Hey2*, *Jag1*, and *EphrinB2*, independent of Cx37 expression (Figure VIIB in the online-only Data Supplement). BMP9 signaling is reported to control mural cell recruitment, indicated by *PDGFβ* and *TGFβ1* expression, contributing to vascular stabilization.[19] Expression of these genes was induced by BMP9 but was unaffected by loss of Cx37 (Figure VIIC in the online-only Data Supplement). We also looked at the SMAD1/5 dependency of these genes and observed various patterns of regulation, with *Hey1/2* and *EphrinB2* showing SMAD1/5-dependent responses to BMP9 under static but not shear stress conditions, while *Jag1* induction by combined BMP9 and shear stress was dependent on SMAD1/5 (Figure VIID in the online-only Data Supplement). *PDGFβ* and *TGFβ* expression by BMP9 under static and shear stress conditions appeared to be only mildly affected by SMAD1/5 levels (Figure VIIE in the online-only Data Supplement).

Cx37 downstream of Notch or BMP9 signaling has been reported to inhibit cell cycling.[19,56] To test this under shear stress conditions, we knocked down Cx37 and sheared cells for 6 hours in complete media. We found no difference in the percent of nuclei that expressed phosphorylated histone 2B (Figure 7A and 7B). This is similar to the finding of Fang et al,[56] who found differences were not present until 12 hours after the onset of flow. We also calculated the average cell size by dividing the area of the field of view by the number of nuclei. However, average cell size was not significantly different (Figure 7C).

Since a key feature of the response to shear stress by ECs is alignment to flow, with the Golgi apparatus located upstream of the nucleus, we examined EC polarization in the presence and absence of Cx37. Because we thought that Cx37 might only delay alignment, but not prevent alignment, we examined the cells after 6 hours of 3.0 Pa shear stress, before full alignment would be present (Figure 7D). We measured the angle from the centre of the Golgi to the centre of the nucleus, relative to the direction of flow (Figure 7E). At this time, neither control nor knockdown ECs showed alignment with flow (Figure 7F).

We then examined the speed and direction of migration of ECs transfected with scrambled siRNA or siRNA targeting *GJA4*. HUVECs were exposed to 0.1 Pa shear stress, a level that we have found to induce the largest amount of migration in our system (unpublished, in preparation). This level of shear stress is within the range observed in zebrafish, avian, and murine embryos during the early phases of vascular remodeling.[38,65,66] We dyed a subset of ECs with CellTracker dye and imaged the cells over 5 hours (Figure 7G). We found that loss of Cx37 did not affect the average migration velocity (Figure 7H). However, we found that *GJA4* knockdown cells had a significantly increased migration with the direction of flow (Figure 7I).

DISCUSSION

Cx37 expression in ECs begins before the onset of blood flow or BMP9/10 expression[55] and is known to be regulated by a number of different factors including KLF2[49] and NOTCH signaling.[56] Here, we have shown that Cx37 expression is inversely regulated by shear stress and BMP9 signaling in a SMAD1/5-dependent manner and that inflammation leads to further disruption of Cx37 expression. We show that vessels enlarge in Cx37-negative regions and that inflammation causes loss of Cx37 in mice with deficient SMAD1/5 signaling. We find that Cx37 is important for directional migration under flow. We propose that, in vasculature already prone to dysregulated EC proliferation and migration due to loss of appropriate SMAD1/5 mechanotransduction, secondary signals such as inflammation induce a further dysregulation of Cx37 expression, which creates a permissive environment for small capillary shunts to enlarge into vascular malformations, such as AVMs.

Our results show profound differences in SMAD1/5 signaling responses under static conditions compared to shear stress conditions. Paradoxically, we find that BMP9/SMAD1/5 signaling in static conditions upregulates Cx37, while under shear stress it becomes downregulated. When SMAD1/5 is knocked down, however, shear stress induces an upregulation of Cx37. We propose that BMP9 strongly activates SMAD1/5 signaling but also weakly activates non-SMAD1/5 signaling, which can also promote Cx37 expression. Both induce Cx37 under static conditions, but under shear stress, we propose that other mechanosensitive transcription factors interact with SMAD1/5, turning a transcriptional activation response into a repression response. This same effect is observed with TGFβ and LDL stimulation. In the absence of SMAD1/5, this transcriptional

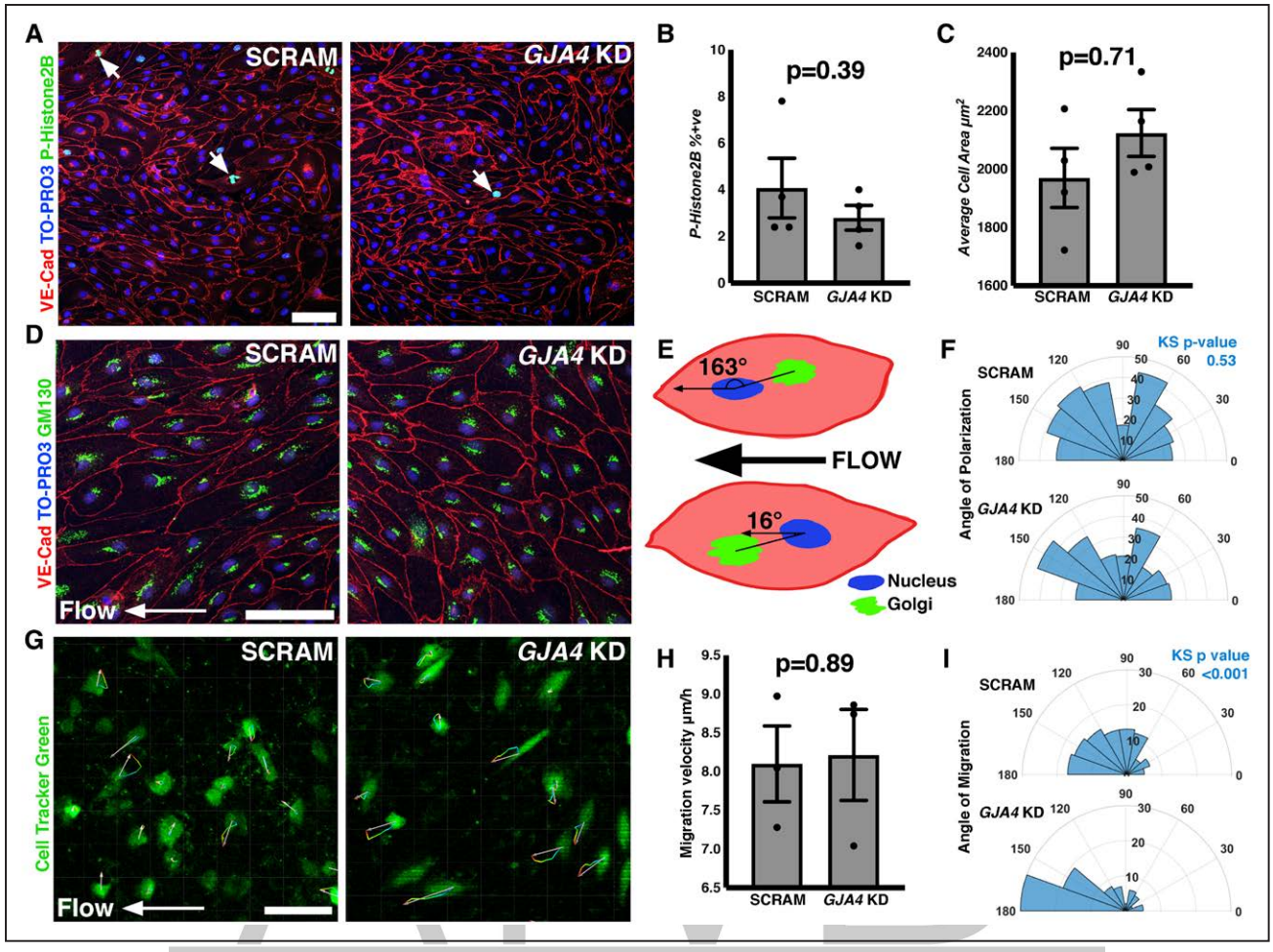

Figure 7. Cx37 (Connexin 37; *GJA4*) is necessary for preventing downstream migration with flow.
A, Phosphorylated histone 2B staining (white arrowheads) in human microvascular endothelial cells (HMvECs) transfected with scrambled siRNA or siRNA against *GJA4* and exposed to 3.0 Pa shear stress for 6 h in complete media. **B**, Quantification of percentage of nuclei positive for phosphorylated histone 2B. n=4 per condition. **C**, Average cell area. n=4 per condition. **D**, Golgi staining in HMvECs transfected with scrambled siRNA or siRNA against *GJA4* and exposed to 3.0 Pa shear stress for 6 h in complete media. **E**, Golgi located upstream of the nucleus had angles of >90°C while Golgi located downstream of the nucleus had angles <90°C. **F**, Rose plot of the angle of the Golgi relative to direction of flow. n=291 cells in scramble condition, 243 cells in GJA4 knockdown condition. **G**, Human umbilical vein endothelial cells (HUVECs) stained with Cell Tracker Green and subjected to 0.1 Pa shear stress for 5 h. Migration was tracked from images every 30 min. **H**, Average velocity of HUVEC migration. **I**, Rose plot of relative direction of migration with respect to flow n=103 cells in scramble, 84 cells in GJA4 knockdown condition. Scale bar = 100 µm. Error bars represent SEM. GM130 indicates golgi marker; KS, Kolmogorov-Smirnov test; P-Histone 2B, phosphorylated histone 2B; TO-PRO3, nuclear marker; and VE-Cad, VE-Cadherin.

repression is lifted and the normally weak non-SMAD1/5 action of BMP9 signaling becomes dominant (Figure 2G). This non-SMAD1/5 signaling could either be mediated via noncanonical BMP signaling or be mediated through other SMADs.

While noncanonical signaling through TGF-β receptors is well understood to affect MAPK, JNK, p38, Ras, ERK, NFκB, and mTOR signaling, among others,[67] comparatively little is known about noncanonical signaling by BMPs under static conditions and is yet unreported under shear stress conditions. BMP9 signaling has been shown to affect Src phosphorylation independently of whether SMAD1/5 activation was disrupted by hyperglycemia,[68] implying a role for noncanonical signaling. Likewise, BMP9/ALK1 signaling was shown to modulate a number of pathways associated with noncanonical TGFβ signaling, including p38/MAPK, PI3K/AKT, and ERK, which were shown to contribute to VEGF-driven vascular hyperplasia in ALK1 heterozygous mice.[25] Neither of these papers explicitly examined the signaling dependence on SMAD1/5; however, these results in combination with our own suggest that the regulation of canonical and noncanonical ALK1 signaling has important implications for AVM formation and HHT.

We also observed that BMP10, as opposed to all other ALK1 ligands tested, cooperates with shear stress to induce, rather than repress, Cx37 expression. If this was mediated through SMAD1/5 signaling, we would expect the same pattern as we observed for the other ligands. We therefore suspect that BMP10 is a stronger activator

of non-SMAD1/5 signaling than BMP9. BMP10 is less discriminatory in its binding to type II receptors than BMP9.[69] BMP9 binds most strongly to ActRIIB, followed by BMPRII and only binds very weakly to ActRIIA, while BMP10 binds all three receptors nearly equally.[69] It is therefore possible that the type II receptor interacting with ALK1 largely determines the balance of SMAD1/5-dependent and independent signaling which will occur. BMPRII, in particular, has been shown to activate non-canonical signaling pathways in response to BMP2.[70] Therefore, the stronger binding of BMP10 to BMPRII could mediate the stronger activation of non-SMAD1/5 signaling, compared to BMP9. The onset of BMP10 expression in the embryonic heart during the remodeling process[41,42,61] may also explain the transition from downregulation of Cx37 in the forming arteries to strong expression of Cx37 in the arteries by E9.5. This, however, remains to be explored.

Here we show that dysregulation of Cx37 downstream of impaired SMAD1/5 mechanotransduction, in combination with the pro-inflammatory molecule TNFα, results in vascular malformations in the yolk sac, directly connecting the dorsal aorta to the inlet of the heart. In several mouse models of disrupted ALK1/Endoglin signaling, wounding has been used to induce AVM formation.[58,71] While wound healing is generally thought of as a neo-angiogenesis model, it also involves a robust inflammatory response, further supporting the role of inflammation in this pathology. In a case report, an HHT patient received an immunosuppressive drug regimen after liver transplantation and experienced a complete resolution of her symptoms.[72] Similarly, thalidomide, which has immunosuppressive properties, reduced symptoms in HHT patients.[73]

An AVM is defined as a direct connection between an artery and a vein, bypassing the capillary bed.[1] Our observed enlarged vessels directly connect the dorsal aorta to inlet to the heart and, as such, are not AVMs per se; however, they have all other characteristics of AVMs that we investigated. We show that this structure is covered by smooth muscle cells over its entire length. We show that the shunt is preferentially perfused; the surrounding capillary bed has little blood flow. We propose that this lack of perfusion is the reason that the vasculature of the dKO^{EC} embryos collapses. Remodeling and shunt formation occur initially, but the lack of flow outside the shunts ultimately causes flow in the yolk sac to stagnate and the vasculature returns to an unremodeled state.

We find that loss of Cx37 promotes downstream migration of ECs, which would allow for accumulation of ECs in post-capillary venules. This mechanism of AVM formation has also been demonstrated in mice with Endoglin loss-of-function.[21] However, mice completely lacking Cx37 are viable and largely normal, although the aorta and carotid arteries do have a larger diameter,[46] and there is a reduction or absence of venous and lymphatic valves.[52,74] AVMs have never been reported for these mice, and we were unable to find any evidence of AVMs or shunts in E9.5 or E10.5 yolk sacs from these mice (Figure VIII in the online-only Data Supplement). Curiously, Cx37-null mice do have increased numbers of collateral vessels.[47] Indeed, Cx37-null mice recover markedly rapidly in hindlimb ligation studies,[75] which requires functional enlargement of these collateral vessels in response to hemodynamic cues (increased blood flow) to restore blood supply to the lower limb. This supports the idea that loss of Cx37 is permissive to enlargement but not sufficient for AVM or shunt formation. The Cx37-null mouse lacks the aspect of abnormal mechanotransduction that is present in our SMAD1/5 dHet^{EC} model and thus is not vulnerable to vascular defect formation.

That loss of Cx37 is permissive to outward remodeling of high flow vessel segments, and formation of vascular enlargements is in agreement with reports that Cx37 is highly expressed by formed arteries, but not at the vascular edge of the developing retina, where labile, not yet perfused capillaries await mechanical cues from flow to instruct their fate.[56] In our model of embryonic vascular remodeling, capillaries distant from the forming artery and vein are stable vessels and therefore express Cx37. The more dynamic areas of the capillary plexus that will undergo remodeling into arteries and veins, equivalent to the sprouting edge of the retina, do not express Cx37, making this a permissive environment for enlargement of the highest flow vessels. Fang and coworkers observed that arteries in the "remodeling zone" of the P6 retina express Cx37, even before coating with smooth muscle cells, while we find that arteries begin to strongly express Cx37 once they have undergone initial enlargement and have become distinguishable from the surrounding capillaries. This difference in timing can be attributed to the presence of high levels of BMP10 in the serum of postnatal mice compared to the early embryo.[41] Furthermore, in *Gja4*$^{-/-}$ P6 retinas, the capillary vessels have a severely dilated phenotype,[56] in agreement with the idea that expression of Cx37 is an important block to flow-induced outward remodeling of the vessel.

In summary, we hypothesize a multistep mechanism of shunt enlargement. In models of impaired SMAD1/5 mechanotransduction, TNFα further decreases Cx37 expression. This area consequently becomes labile and permissive to vessel enlargement. In capillary segments with slightly higher flow, hemodynamic cues are then able to instruct the formation of shunts, and the aberrant proliferative and migratory behavior of ECs with disrupted SMAD1/5 signaling, combined with the downstream migration of ECs lacking Cx37, in response to flow, allows for shunt enlargement.

ARTICLE INFORMATION

Received May 14, 2019; accepted January 22, 2020.

Affiliations

From the Department of Cardiovascular Sciences, Centre for Molecular and Vascular Biology (H.M.P., A.T., N.C., A.Z., E.A.V.J.) and Lab of Developmental Neurobiology (A.D.), KU Leuven, Belgium; Leeds Institute of Cardiovascular and Metabolic Medicine, School of Medicine, University of Leeds, United Kingdom (V.C.); Department of Medicine, Centre Hospitalier Universitaire Vaudois, University of Lausanne, Switzerland (L.H., J.-A.H.); and Department of Pathology and Immunology, University of Geneva, Switzerland (B.R.K.).

Acknowledgments

We thank Dr Janis Burt for providing the Cx37 antibody. We thank Marleen Lox, Petra Vandervoort, Nadèche Geuens, Steven Simmonds, Ilona Cuijpers, Paolo Carai, Ljuba Ponomarev, and Chantal Thys for assistance with experimental work.

Sources of Funding

H.M. Peacock was supported by an NSERC Post Graduate Scholarship (459882) and by an FWO Aspirant mandate (11ZD516N). N. Criem was supported by an FWO Aspirant mandate (1127815 N). V. Caolo was supported by an FWO Fellowship (12T2815N). A. Deryckere was supported by an SB PhD fellowship from the FWO (1S19517N). J.-A. Haefliger was supported by grants from the SNF (31003A-175452/1) and the Swiss Cancer League (KFS-3796-02-2016). B.R. Kwak was supported by the SNF (310030_162579). A. Zwijsen was supported by C1 Internal Funding from KU Leuven (C1-12/16/023). E.A.V. Jones was supported by a grant from the Life Science Research Partners, C1 Internal Funding from KU Leuven (C1-12/16/019), an ERA-Net grant (LYMIT-Dis) and an FWO research project grant (G091018N).

Disclosures

None.

Supplemental Materials

Major Resources Table
Materials and Methods
Figure I–VIII
Movies I and II

REFERENCES

1. Peacock HM, Caolo V, Jones EA. Arteriovenous malformations in hereditary haemorrhagic telangiectasia: looking beyond ALK1-NOTCH interactions. *Cardiovasc Res*. 2016;109:196–203. doi: 10.1093/cvr/cvv264
2. Wooderchak-Donahue WL, McDonald J, O'Fallon B, Upton PD, Li W, Roman BL, Young S, Plant P, Fülöp GT, Langa C, et al. BMP9 mutations cause a vascular-anomaly syndrome with phenotypic overlap with hereditary hemorrhagic telangiectasia. *Am J Hum Genet*. 2013;93:530–537. doi: 10.1016/j.ajhg.2013.07.004
3. Gallione CJ, Repetto GM, Legius E, Rustgi AK, Schelley SL, Tejpar S, Mitchell G, Drouin E, Westermann CJ, Marchuk DA. A combined syndrome of juvenile polyposis and hereditary haemorrhagic telangiectasia associated with mutations in MADH4 (SMAD4). *Lancet*. 2004;363:852–859. doi: 10.1016/S0140-6736(04)15732-2
4. Johnson DW, Berg JN, Baldwin MA, Gallione CJ, Marondel I, Yoon SJ, Stenzel TT, Speer M, Pericak-Vance MA, Diamond A, et al. Mutations in the activin receptor-like kinase 1 gene in hereditary haemorrhagic telangiectasia type 2. *Nat Genet*. 1996;13:189–195. doi: 10.1038/ng0696-189
5. McAllister KA, Grogg KM, Johnson DW, Gallione CJ, Baldwin MA, Jackson CE, Helmbold EA, Markel DS, McKinnon WC, Murrell J. Endoglin, a TGF-beta binding protein of endothelial cells, is the gene for hereditary haemorrhagic telangiectasia type 1. *Nat Genet*. 1994;8:345–351. doi: 10.1038/ng1294-345
6. Seki T, Yun J, Oh SP. Arterial endothelium-specific activin receptor-like kinase 1 expression suggests its role in arterialization and vascular remodeling. *Circ Res*. 2003;93:682–689. doi: 10.1161/01.RES.0000095246.40391.3B
7. Lebrin F, Goumans MJ, Jonker L, Carvalho RL, Valdimarsdottir G, Thorikay M, Mummery C, Arthur HM, ten Dijke P. Endoglin promotes endothelial cell proliferation and TGF-beta/ALK1 signal transduction. *EMBO J*. 2004;23:4018–4028. doi: 10.1038/sj.emboj.7600386
8. Itoh F, Itoh S, Goumans MJ, Valdimarsdottir G, Iso T, Dotto GP, Hamamori Y, Kedes L, Kato M, ten Dijke Pt P. Synergy and antagonism between notch and BMP receptor signaling pathways in endothelial cells. *EMBO J*. 2004;23:541–551. doi: 10.1038/sj.emboj.7600065
9. Scharpfenecker M, van Dinther M, Liu Z, van Bezooijen RL, Zhao Q, Pukac L, Löwik CW, ten Dijke P. BMP-9 signals via ALK1 and inhibits bFGF-induced endothelial cell proliferation and VEGF-stimulated angiogenesis. *J Cell Sci*. 2007;120(pt 6):964–972. doi: 10.1242/jcs.002949
10. Somekawa S, Imagawa K, Hayashi H, Sakabe M, Ioka T, Sato GE, Inada K, Iwamoto T, Mori T, Uemura S, et al. Tmem100, an ALK1 receptor signaling-dependent gene essential for arterial endothelium differentiation and vascular morphogenesis. *Proc Natl Acad Sci U S A*. 2012;109:12064–12069. doi: 10.1073/pnas.1207210109
11. Vandersmissen I, Craps S, Depypere M, Coppiello G, van Gastel N, Maes F, Carmeliet G, Schrooten J, Jones EA, Umans L, et al. Endothelial Msx1 transduces hemodynamic changes into an arteriogenic remodeling response. *J Cell Biol*. 2015;210:1239–1256. doi: 10.1083/jcb.201502003
12. Nolan-Stevaux O, Zhong W, Culp S, Shaffer K, Hoover J, Wickramasinghe D, Ruefli-Brasse A. Endoglin requirement for BMP9 signaling in endothelial cells reveals new mechanism of action for selective anti-endoglin antibodies. *PLoS One*. 2012;7:e50920. doi: 10.1371/journal.pone.0050920
13. Arnold SJ, Maretto S, Islam A, Bikoff EK, Robertson EJ. Dose-dependent smad1, smad5 and smad8 signaling in the early mouse embryo. *Dev Biol*. 2006;296:104–118. doi: 10.1016/j.ydbio.2006.04.442
14. Li DY, Sorensen LK, Brooke BS, Urness LD, Davis EC, Taylor DG, Boak BB, Wendel DP. Defective angiogenesis in mice lacking endoglin. *Science*. 1999;284:1534–1537. doi: 10.1126/science.284.5419.1534
15. Moya IM, Umans L, Maas E, Pereira PN, Beets K, Francis A, Sents W, Robertson EJ, Mummery CL, Huylebroeck D, et al. Stalk cell phenotype depends on integration of notch and smad1/5 signaling cascades. *Dev Cell*. 2012;22:501–514. doi: 10.1016/j.devcel.2012.01.007
16. Oh SP, Seki T, Goss KA, Imamura T, Yi Y, Donahoe PK, Li L, Miyazono K, ten Dijke P, Kim S, et al. Activin receptor-like kinase 1 modulates transforming growth factor-beta 1 signaling in the regulation of angiogenesis. *Proc Natl Acad Sci U S A*. 2000;97:2626–2631. doi: 10.1073/pnas.97.6.2626
17. Oshima M, Oshima H, Taketo MM. TGF-beta receptor type II deficiency results in defects of yolk sac hematopoiesis and vasculogenesis. *Dev Biol*. 1996;179:297–302. doi: 10.1006/dbio.1996.0259
18. Arthur HM, Ure J, Smith AJ, Renforth G, Wilson DI, Torsney E, Charlton R, Parums DV, Jowett T, Marchuk DA, et al. Endoglin, an ancillary TGFbeta receptor, is required for extraembryonic angiogenesis and plays a key role in heart development. *Dev Biol*. 2000;217:42–53. doi: 10.1006/dbio.1999.9534
19. Baeyens N, Larrivée B, Ola R, Hayward-Piatkowskyi B, Dubrac A, Huang B, Ross TD, Coon BG, Min E, Tsarfati M, et al. Defective fluid shear stress mechanotransduction mediates hereditary hemorrhagic telangiectasia. *J Cell Biol*. 2016;214:807–816. doi: 10.1083/jcb.201603106
20. Baeyens N, Bandyopadhyay C, Coon BG, Yun S, Schwartz MA. Endothelial fluid shear stress sensing in vascular health and disease. *J Clin Invest*. 2016;126:821–828. doi: 10.1172/JCI83083
21. Jin Y, Muhl L, Burmakin M, Wang Y, Duchez AC, Betsholtz C, Arthur HM, Jakobsson L. Endoglin prevents vascular malformation by regulating flow-induced cell migration and specification through VEGFR2 signalling. *Nat Cell Biol*. 2017;19:639–652. doi: 10.1038/ncb3534
22. Poduri A, Chang AH, Raftrey B, Rhee S, Van M, Red-Horse K. Endothelial cells respond to the direction of mechanical stimuli through SMAD signaling to regulate coronary artery size. *Development*. 2017;144:3241–3252. doi: 10.1242/dev.150904
23. Sugden WW, Meissner R, Aegerter-Wilmsen T, Tsaryk R, Leonard EV, Bussmann J, Hamm MJ, Herzog W, Jin Y, Jakobsson L, et al. Endoglin controls blood vessel diameter through endothelial cell shape changes in response to haemodynamic cues. *Nat Cell Biol*. 2017;19:653–665. doi: 10.1038/ncb3528
24. Vion AC, Alt S, Klaus-Bergmann A, Szymborska A, Zheng T, Perovic T, Hammoutene A, Oliveira MB, Bartels-Klein E, Hollfinger I, et al. Primary cilia sensitize endothelial cells to BMP and prevent excessive vascular regression. *J Cell Biol*. 2018;217:1651–1665. doi: 10.1083/jcb.201706151
25. Alsina-Sanchís E, García-Ibáñez Y, Figueiredo AM, Riera-Domingo C, Figueras A, Matias-Guiu X, Casanovas O, Botella LM, Pujana MA, Riera-Mestre A, et al. ALK1 loss results in vascular hyperplasia in mice and humans through PI3K activation. *Arterioscler Thromb Vasc Biol*. 2018;38:1216–1229. doi: 10.1161/ATVBAHA.118.310760
26. Rochon ER, Menon PG, Roman BL. Alk1 controls arterial endothelial cell migration in lumenized vessels. *Development*. 2016;143:2593–2602. doi: 10.1242/dev.135392
27. HannonLab. Fastx-toolkit. Available at: http://hannonlabcshledu/fastx_toolkit/indexhtml. 2010.
28. Martin M. Cutadapt removes adapter sequences from high-throughput sequencing reads. *EMBO J*. 2011;17:10–12.

29. Morgan M, Anders S, Lawrence M, Aboyoun P, Pagès H, Gentleman R. ShortRead: a bioconductor package for input, quality assessment and exploration of high-throughput sequence data. *Bioinformatics*. 2009;25:2607–2608. doi: 10.1093/bioinformatics/btp450
30. Langmead B, Salzberg SL. Fast gapped-read alignment with Bowtie 2. *Nat Methods*. 2012;9:357–359. doi: 10.1038/nmeth.1923
31. Dobin A, Davis CA, Schlesinger F, Drenkow J, Zaleski C, Jha S, Batut P, Chaisson M, Gingeras TR. STAR: ultrafast universal RNA-seq aligner. *Bioinformatics*. 2013;29:15–21. doi: 10.1093/bioinformatics/bts635
32. Li H, Handsaker B, Wysoker A, Fennell T, Ruan J, Homer N, Marth G, Abecasis G, Durbin R; 1000 Genome Project Data Processing Subgroup. The sequence alignment/map format and SAMtools. *Bioinformatics*. 2009;25:2078–2079. doi: 10.1093/bioinformatics/btp352
33. Liao Y, Smyth GK, Shi W. featureCounts: an efficient general purpose program for assigning sequence reads to genomic features. *Bioinformatics*. 2014;30:923–930. doi: 10.1093/bioinformatics/btt656
34. Risso D, Schwartz K, Sherlock G, Dudoit S. GC-content normalization for RNA-Seq data. *BMC Bioinformatics*. 2011;12:480. doi: 10.1186/1471-2105-12-480
35. Robinson MD, Smyth GK. Moderated statistical tests for assessing differences in tag abundance. *Bioinformatics*. 2007;23:2881–2887. doi: 10.1093/bioinformatics/btm453
36. Benjamini Y, Hochberg Y. Controlling the false discovery rate: a practical and powerful approach to multiple testing. *J R Stat Soc Ser B*. 1995;57:289–300.
37. Jones EA, Crotty D, Kulesa PM, Waters CW, Baron MH, Fraser SE, Dickinson ME. Dynamic *in vivo* imaging of postimplantation mammalian embryos using whole embryo culture. *Genesis*. 2002;34:228–235. doi: 10.1002/gene.10162
38. Ghaffari S, Leask RL, Jones EA. Simultaneous imaging of blood flow dynamics and vascular remodelling during development. *Development*. 2015;142:4158–4167. doi: 10.1242/dev.127019
39. Kraehling JR, Chidlow JH, Rajagopal C, Sugiyama MG, Fowler JW, Lee MY, Zhang X, Ramírez CM, Park EJ, Tao B, et al. Genome-wide RNAi screen reveals ALK1 mediates LDL uptake and transcytosis in endothelial cells. *Nat Commun*. 2016;7:13516. doi: 10.1038/ncomms13516
40. Cunha SI, Pardali E, Thorikay M, Anderberg C, Hawinkels L, Goumans MJ, Seehra J, Heldin CH, ten Dijke P, Pietras K. Genetic and pharmacological targeting of activin receptor-like kinase 1 impairs tumor growth and angiogenesis. *J Exp Med*. 2010;207:85–100. doi: 10.1084/jem.20091309
41. Chen H, Brady Ridgway J, Sai T, Lai J, Warming S, Chen H, Roose-Girma M, Zhang G, Shou W, Yan M. Context-dependent signaling defines roles of BMP9 and BMP10 in embryonic and postnatal development. *Proc Natl Acad Sci U S A*. 2013;110:11887–11892. doi: 10.1073/pnas.1306074110
42. Neuhaus H, Rosen V, Thies RS. Heart specific expression of mouse BMP-10 a novel member of the TGF-beta superfamily. *Mech Dev*. 1999;80:181–184. doi: 10.1016/s0925-4773(98)00221-4
43. Tang AT, Choi JP, Kotzin JJ, Yang Y, Hong CC, Hobson N, Girard R, Zeineddine HA, Lightle R, Moore T, et al. Endothelial TLR4 and the microbiome drive cerebral cavernous malformations. *Nature*. 2017;545:305–310. doi: 10.1038/nature22075
44. Jacobsen NL, Pontifex TK, Li H, Solan JL, Lampe PD, Sorgen PL, Burt JM. Regulation of Cx37 channel and growth-suppressive properties by phosphorylation. *J Cell Sci*. 2017;130:3308–3321. doi: 10.1242/jcs.202572
45. Morel S, Burnier L, Roatti A, Chassot A, Roth I, Sutter E, Galan K, Pfenniger A, Chanson M, Kwak BR. Unexpected role for the human Cx37 C1019T polymorphism in tumour cell proliferation. *Carcinogenesis*. 2010;31:1922–1931. doi: 10.1093/carcin/bgq170
46. Allagnat F, Dubuis C, Lambelet M, Le Gal L, Alonso F, Corpataux JM, Déglise S, Haefliger JA. Connexin37 reduces smooth muscle cell proliferation and intimal hyperplasia in a mouse model of carotid artery ligation. *Cardiovasc Res*. 2017;113:805–816. doi: 10.1093/cvr/cvx079
47. Fang JS, Angelov SN, Simon AM, Burt JM. Cx37 deletion enhances vascular growth and facilitates ischemic limb recovery. *Am J Physiol Heart Circ Physiol*. 2011;301:H1872–H1881. doi: 10.1152/ajpheart.00683.2011
48. Pries AR, Höpfner M, le Noble F, Dewhirst MW, Secomb TW. The shunt problem: control of functional shunting in normal and tumour vasculature. *Nat Rev Cancer*. 2010;10:587–593. doi: 10.1038/nrc2895
49. Pfenniger A, Wong C, Sutter E, Cuhlmann S, Dunoyer-Geindre S, Mach F, Horrevoets AJ, Evans PC, Krams R, Kwak BR. Shear stress modulates the expression of the atheroprotective protein Cx37 in endothelial cells. *J Mol Cell Cardiol*. 2012;53:299–309. doi: 10.1016/j.yjmcc.2012.05.011
50. Haefliger JA, Polikar R, Schnyder G, Burdet M, Sutter E, Pexieder T, Nicod P, Meda P. Connexin37 in normal and pathological development of mouse heart and great arteries. *Dev Dyn*. 2000;218:331–344. doi: 10.1002/(SICI)1097-0177(200006)218:2<331::AID-DVDY7>3.0.CO;2-4
51. Kwak BR, Mulhaupt F, Veillard N, Gros DB, Mach F. Altered pattern of vascular connexin expression in atherosclerotic plaques. *Arterioscler Thromb Vasc Biol*. 2002;22:225–230. doi: 10.1161/hq0102.104125
52. Sabine A, Agalarov Y, Maby-El Hajjami H, Jaquet M, Hägerling R, Pollmann C, Bebber D, Pfenniger A, Miura N, Dormond O, et al. Mechanotransduction, PROX1, and FOXC2 cooperate to control connexin37 and calcineurin during lymphatic-valve formation. *Dev Cell*. 2012;22:430–445. doi: 10.1016/j.devcel.2011.12.020
53. Kanady JD, Munger SJ, Witte MH, Simon AM. Combining foxc2 and Connexin37 deletions in mice leads to severe defects in lymphatic vascular growth and remodeling. *Dev Biol*. 2015;405:33–46. doi: 10.1016/j.ydbio.2015.06.004
54. Lucitti JL, Jones EA, Huang C, Chen J, Fraser SE, Dickinson ME. Vascular remodeling of the mouse yolk sac requires hemodynamic force. *Development*. 2007;134:3317–3326. doi: 10.1242/dev.02883
55. Chong DC, Koo Y, Xu K, Fu S, Cleaver O. Stepwise arteriovenous fate acquisition during mammalian vasculogenesis. *Dev Dyn*. 2011;240:2153–2165. doi: 10.1002/dvdy.22706
56. Fang JS, Coon BG, Gillis N, Chen Z, Qiu J, Chittenden TW, Burt JM, Schwartz MA, Hirschi KK. Shear-induced Notch-Cx37-p27 axis arrests endothelial cell cycle to enable arterial specification. *Nat Commun*. 2017;8:2149. doi: 10.1038/s41467-017-01742-7
57. Tual-Chalot S, Oh SP, Arthur HM. Mouse models of hereditary hemorrhagic telangiectasia: recent advances and future challenges. *Front Genet*. 2015;6:25. doi: 10.3389/fgene.2015.00025
58. Garrido-Martin EM, Nguyen HL, Cunningham TA, Choe SW, Jiang Z, Arthur HM, Lee YJ, Oh SP. Common and distinctive pathogenetic features of arteriovenous malformations in hereditary hemorrhagic telangiectasia 1 and hereditary hemorrhagic telangiectasia 2 animal models–brief report. *Arterioscler Thromb Vasc Biol*. 2014;34:2232–2236. doi: 10.1161/ATVBAHA.114.303984
59. Kwak BR, Pepper MS, Gros DB, Meda P. Inhibition of endothelial wound repair by dominant negative connexin inhibitors. *Mol Biol Cell*. 2001;12:831–845. doi: 10.1091/mbc.12.4.831
60. van Rijen HV, van Kempen MJ, Postma S, Jongsma HJ. Tumour necrosis factor alpha alters the expression of connexin43, connexin40, and connexin37 in human umbilical vein endothelial cells. *Cytokine*. 1998;10:258–264. doi: 10.1006/cyto.1997.0287
61. Chen H, Shi S, Acosta L, Li W, Lu J, Bao S, Chen Z, Yang Z, Schneider MD, Chien KR, et al. BMP10 is essential for maintaining cardiac growth during murine cardiogenesis. *Development*. 2004;131:2219–2231. doi: 10.1242/dev.01094
62. Corada M, Morini MF, Dejana E. Signaling pathways in the specification of arteries and veins. *Arterioscler Thromb Vasc Biol*. 2014;34:2372–2377. doi: 10.1161/ATVBAHA.114.303218
63. Foty RA, Steinberg MS. The differential adhesion hypothesis: a direct evaluation. *Dev Biol*. 2005;278:255–263. doi: 10.1016/j.ydbio.2004.11.012
64. Simon AM, Chen H, Jackson CL. Cx37 and Cx43 localize to zona pellucida in mouse ovarian follicles. *Cell Commun Adhes*. 2006;13:61–77. doi: 10.1080/15419060600631748
65. Karthik S, Djukic T, Kim JD, Zuber B, Makanya A, Odriozola A, Hlushchuk R, Filipovic N, Jin SW, Djonov V. Synergistic interaction of sprouting and intussusceptive angiogenesis during zebrafish caudal vein plexus development. *Sci Rep*. 2018;8:9840. doi: 10.1038/s41598-018-27791-6
66. Jones EA, Baron MH, Fraser SE, Dickinson ME. Measuring hemodynamic changes during mammalian development. *Am J Physiol Heart Circ Physiol*. 2004;287:H1561–H1569. doi: 10.1152/ajpheart.00081.2004
67. Zhang YE. Non-smad signaling pathways of the TGF-beta Family. *Cold Spring Harb Perspect Biol*. 2017;9. doi: 10.1101/cshperspect.a022129
68. Akla N, Viallard C, Popovic N, Lora Gil C, Sapieha P, Larrivée B. BMP9 (Bone Morphogenetic Protein-9)/Alk1 (Activin-Like Kinase Receptor Type I) signaling prevents hyperglycemia-induced vascular permeability. *Arterioscler Thromb Vasc Biol*. 2018;38:1821–1836. doi: 10.1161/ATVBAHA.118.310733
69. Townson SA, Martinez-Hackert E, Greppi C, Lowden P, Sako D, Liu J, Ucran JA, Liharska K, Underwood KW, Seehra J, et al. Specificity and structure of a high affinity activin receptor-like kinase 1 (ALK1) signaling complex. *J Biol Chem*. 2012;287:27313–27325. doi: 10.1074/jbc.M112.377960
70. de Jesus Perez VA, Alastalo TP, Wu JC, Axelrod JD, Cooke JP, Amieva M, Rabinovitch M. Bone morphogenetic protein 2 induces pulmonary angiogenesis via Wnt-beta-catenin and Wnt-RhoA-Rac1 pathways. *J Cell Biol*. 2009;184:83–99. doi: 10.1083/jcb.200806049

71. Gkatzis K, Thalgott J, Dos-Santos-Luis D, Martin S, Lamandé N, Carette MF, Disch F, Snijder RJ, Westermann CJ, Mager JJ, et al. Interaction between ALK1 signaling and connexin40 in the development of arteriovenous malformations. *Arterioscler Thromb Vasc Biol.* 2016;36:707–717. doi: 10.1161/ATVBAHA.115.306719
72. McAlister VC. Regression of cutaneous and gastrointestinal telangiectasia with sirolimus and aspirin in a patient with hereditary hemorrhagic telangiectasia. *Ann Intern Med.* 2006;144:226–7. doi: 10.7326/0003-4819-144-3-200602070-00030
73. Lebrin F, Srun S, Raymond K, Martin S, van den Brink S, Freitas C, Bréant C, Mathivet T, Larrivée B, Thomas JL, et al. Thalidomide stimulates vessel maturation and reduces epistaxis in individuals with hereditary hemorrhagic telangiectasia. *Nat Med.* 2010;16:420–428. doi: 10.1038/nm.2131
74. Kanady JD, Dellinger MT, Munger SJ, Witte MH, Simon AM. Connexin37 and connexin43 deficiencies in mice disrupt lymphatic valve development and result in lymphatic disorders including lymphedema and chylothorax. *Dev Biol.* 2011;354:253–266. doi: 10.1016/j.ydbio.2011.04.004
75. Fang JS, Angelov SN, Simon AM, Burt JM. Cx40 is required for, and cx37 limits, postischemic hindlimb perfusion, survival and recovery. *J Vasc Res.* 2012;49:2–12. doi: 10.1159/000329616